

1 Simulating *Ips typographus* (L.), outbreak dynamics and their 2 influence on carbon balance estimates with ORCHIDEE r8627

3

4 Guillaume Marie^{1*}, Jina Jeong^{2*}, Hervé Jactel³, Gunnar Petter⁴, Maxime Cailleret⁵, Matthew J.
5 McGrath¹, Vladislav Bastrikov⁶, Josefina Ghattas⁷, Bertrand Guenet⁸, Anne Sofie Lansø⁹, Kim
6 Naudts¹¹, Aude Valade¹⁰, Chao Yue¹², Sebastiaan Luyssaert²

7

8 ¹ Laboratoire des Sciences du Climat et de l'Environnement, CEA CNRS UVSQ UP Saclay, 91191 Orme des
9 Merisiers, Gif-sur-Yvette, France

10 ² Faculty of Science, A-LIFE, Vrije Universiteit Amsterdam, 1081 BT Amsterdam, the Netherlands

11 ³ INRAE, University of Bordeaux, UMR Biogeco, 33612 Cestas, France

12 ⁴ ETH Zürich, Department of Environmental Systems Science, Forest Ecology, 8092 Zürich, Switzerland

13 ⁵ INRAE, Aix-Marseille Univ, UMR RECOVER, 13182 Aix-en-Provence, France

14 ⁶ Science Partner, France

15 ⁷ Institut Pierre-Simon Laplace – Sciences du climat (IPSL), 75105 Jussieu, France

16 ⁸ Laboratoire de Géologie, Ecole Normale Supérieure, CNRS, PSL Research University, IPSL, 75005 Paris, France

17 ⁹ Department of Environmental Science, Aarhus Universitet, Frederiksborgvej 399, 4000 Roskilde, Denmark

18 ¹⁰ Eco & Sols, Univ Montpellier, CIRAD, INRAE, 34060 Institut Agro, IRD, Montpellier, France

19 ¹¹ Department of Earth Sciences, Vrije Universiteit Amsterdam, 1081 HV Amsterdam, the Netherlands

20 ¹² State Key Laboratory of Soil Erosion and Dryland Farming on the Loess Plateau, Northwest A & F University,
21 Yangling, Shaanxi, China

22

23 * These authors contributed equally to this study

24

25 **Corresponding author:** Guillaume Marie, guillaume.marie@lsce.ipsl.fr, Jina Jeong, j.jeong@vu.nl, Sebastiaan
26 Luyssaert, s.luyssaert@vu.nl

27

28 **Abstract** : New (a)biotic conditions resulting from climate change are expected to change disturbance dynamics,
29 such as windthrow, forest fires, droughts, and insect outbreaks, and their interactions. These unprecedented natural
30 disturbance dynamics might alter the capability of forest ecosystems to buffer atmospheric CO₂ increases, potentially
31 leading forests to transform from sinks into sources of CO₂. This study aims to enhance the ORCHIDEE land surface
32 model to study the impacts of climate change on the dynamics of the bark beetle *Ips typographus* and subsequent
33 effects on forest functioning. The *Ips typographus* outbreak model is inspired by previous work from Temperli et al.
34 2013 for the LandClim landscape model. The new implementation of this model in ORCHIDEE r8627 accounts for
35 key differences between ORCHIDEE and LandClim: (1) the coarser spatial resolution of ORCHIDEE, (2) the higher

36 temporal resolution of ORCHIDEE, and (3) the pre-existing process representation of windthrow, drought, and forest
37 structure in ORCHIDEE. Simulation experiments demonstrated the capability of ORCHIDEE to simulate a variety
38 of post-disturbance forest dynamics observed in empirical studies. Through an array of simulation experiments
39 across various climatic conditions and windthrow intensities, the model was tested for its sensitivity to climate,
40 initial disturbance, and selected parameter values. The results of these tests indicated that with a single set of
41 parameters, ORCHIDEE outputs spanned the range of observed dynamics. Additional tests highlighted the
42 substantial impact of incorporating *Ips typographus* outbreaks on carbon dynamics. Notably, the study revealed that
43 modeling abrupt mortality events, as opposed to a continuous mortality framework, provides new insights into the
44 short-term carbon sequestration potential of forests under disturbance regimes by showing that the continuous
45 mortality framework tends to overestimate the carbon sink capacity of forests in the 20 to 50 year range in
46 ecosystems under high disturbance pressure, compared to scenarios with abrupt mortality events. This model
47 enhancement underscores the critical need to include disturbance dynamics in land surface models to refine
48 predictions of forest carbon dynamics in a changing climate.

49

50 1. Introduction

51 Future climate will likely bring new abiotic constraints through the co-occurrence of multiple connected hazards,
52 e.g., “hotter droughts”, which are droughts combined with heat waves (Allen et al., 2015; Zscheischler et al., 2018),
53 but also new biotic conditions from interacting natural and anthropogenic disturbances, e.g., insect outbreaks
54 following windthrow or forest fires (Seidl et al., 2017). Unprecedented natural disturbance dynamics might alter
55 biogeochemical cycles specifically the capability of forest ecosystems to buffer the CO₂ increase in the atmosphere
56 (Hicke et al., 2012; Seidl et al., 2014) and the risk that forests are transformed from sinks into sources of CO₂ (Kurz
57 et al., 2008a). The magnitude of such alteration, however, remains uncertain principally due to the lack of impact
58 studies that include disturbance regime shifts at global scale (Seidl et al., 2011).

59

60 Land surface models are used to study the relationships between climate change and the biogeochemical cycles of
61 carbon, water, and nitrogen (Ciais et al., 2005; Cox et al., 2000; Friedlingstein et al., 2006; Luysaert et al., 2018;
62 Zaehle and Dalmonech, 2011). Many of these models use background mortality to obtain an equilibrium in their
63 biomass pools. This classic approach towards forest dynamics, which assumes steady-state conditions over long
64 periods of time, may not be suitable for assessing the impacts of disturbances on shorter time scales under a fast
65 changing climate. This could be considered a shortcoming in the land surface models because disturbances can have
66 significant impacts on ecosystem services, such as water regulation, carbon sequestration, and biodiversity (Quillet
67 et al., 2010). Mechanistic approaches that account for a variety of mortality causes, such as age, size, competition,
68 climate, and disturbances, are now being considered and tested to simulate forest dynamics more accurately
69 (Migliavacca et al., 2021). For example, the land surface model ORCHIDEE accounts for mortality from
70 interspecific competition for light in addition to background mortality (Naudts et al., 2015). Implementing a more
71 mechanistic view on mortality is thought to be essential for improving our understanding of the impacts of climate
72 change on forest dynamics and the provision of ecosystem services.

73

74 Land surface models also face the challenge of better describing mortality particularly when it comes to ecosystem
75 responses to “cascading disturbances”, where legacy effects from one disturbance affect the next (Buma, 2015;
76 Zscheischler et al., 2018). Biotic disturbances, such as bark beetle outbreaks, strongly depend on previous
77 disturbances as their infestation capabilities are higher when tree vitality is low, for example following drought or
78 storm events (Seidl et al., 2018). This illustrates how interactions between biotic and abiotic disturbances can have
79 substantial effects on ecosystem dynamics and must be accounted for in land surface models to improve our
80 understanding of the impacts of climate change on forest dynamics (Seidl et al., 2011; Temperli et al., 2013a). While
81 progress has been made towards including abrupt mortality from individual disturbance types such as wildfire
82 (Lasslop et al., 2014; Migliavacca et al., 2013; Yue et al., 2014), windthrow (Chen et al., 2018) and drought (Yao et
83 al., 2022), the interaction of biotic and abiotic disturbances remains both a knowledge and modeling gap (Kautz et
84 al., 2018).

85

86 Bark beetle infestations are increasingly recognized as disturbance events of regional to global importance (Bentz et
87 al., 2010; Kurz et al., 2008b; Seidl et al., 2018). Notably, a bark beetle outbreak ravaged over 90% of Engelmann
88 spruce trees across approximately 325,000 hectares in the Canadian and American Rocky Mountains between 2005
89 and 2017 (Andrus et al., 2020). In Europe, the bark beetle *Ips typographus* has been involved in up to 8% of total
90 tree mortality due to natural disturbances from 1850 to 2000 (Hlásny et al., 2021a). A recent increase in beetle
91 activity, particularly following mild winters (Andrus et al., 2020; Kurz et al., 2008c), windthrow (Mezei et al., 2017),
92 and droughts (Nardi et al., 2023) have been well-documented (Hlásny et al., 2021a; Pasztor et al., 2014),
93 underscoring the need to integrate bark beetle dynamics into land surface modeling.

94

95 Past studies used a variety of approaches to model the impacts of bark beetles on forests. While some models treated
96 bark beetle outbreaks as background mortality (Luyssaert et al., 2018; Naudts et al., 2016), others dynamically
97 modeled these outbreaks within ecosystems (Jönsson et al., 2012; Seidl and Rammer, 2016; Temperli et al., 2013b).
98 Studies with prescribed beetle outbreaks tend to focus on the direct effects of the outbreak on forest conditions and
99 carbon fluxes, but are likely to overlook more complex feedback processes, such as interactions with other
100 disturbances and longer-term impacts. Conversely, dynamic modeling of beetle outbreaks, provides a more
101 comprehensive view by incorporating the lifecycle of bark beetles, tree defense mechanisms, and ensuing alterations
102 in forest composition and functionality.

103

104 Simulation experiments for *Ips typographus* outbreaks using the LPJ-GUESS vegetation model highlighted regional
105 variations in outbreak frequencies, pinpointing climate change as a key exacerbating factor (Jönsson et al., 2012).
106 Simulation experiments with the iLand landscape model suggested that almost 65% of *Ips typographus* outbreaks are
107 aggravated by other environmental drivers (Seidl and Rammer, 2016). A 4°C temperature increase could result in a
108 265% increase in disturbed area and a 1800% growth in the average patch size of the disturbance (Seidl and Rammer
109 2016). Disturbance interactions were ten times more sensitive to temperature changes, boosting the disturbance

110 regime's climate sensitivity. The results of these studies justify the inclusion of interacting disturbances in land
111 surface models, such as ORCHIDEE, which are used in future climate predictions and impact studies (Boucher et al.,
112 2020).

113

114 The objectives of this study are: (1) to develop and implement a spatially implicit outbreak model for *Ips*
115 *typographus* in the land surface model ORCHIDEE inspired by the work from Temperli et al. (2013), and (2) use
116 simulation experiments to characterize the behavior of this newly added model functionality.

117

118 2. Model description

119 2.1. The land surface model ORCHIDEE

120 ORCHIDEE is the land surface model of the IPSL (Institut Pierre Simon Laplace) Earth system model (Boucher et
121 al., 2020; Krinner et al., 2005). ORCHIDEE can, however, also be run uncoupled as a stand-alone land surface
122 model forced by temperature, humidity, pressure, precipitation, and wind fields. Unlike the coupled setup, which
123 needs to run on the global scale, the stand-alone configuration can cover any area ranging from a single grid point to
124 the global domain. In this study ORCHIDEE was run as a stand-alone land surface model.

125

126 ORCHIDEE does not enforce any particular spatial resolution. The spatial resolution is an implicit user setting that
127 is determined by the resolution of the climate forcing (or the resolution of the atmospheric model in a coupled
128 configuration). ORCHIDEE can run on any temporal resolution. This apparent flexibility is somewhat restricted as
129 processes are formalized at given time steps: half-hourly (e.g., photosynthesis and energy budget), daily (i.e., net
130 primary production), and annual (i.e. vegetation demographic processes). With the current model architecture
131 meaningful simulations should have a temporal resolution of one minute to one hour for the calculation of energy
132 balance, water balance, and photosynthesis.

133

134 ORCHIDEE utilizes meta-classes to discretize the global diversity in vegetation. The model includes 13
135 meta-classes by default, including one class for bare soil, eight classes for various combinations of leaf-type and
136 climate zones of forests, two classes for grasslands, and two classes for croplands. Each meta-class can be further
137 subdivided into an unlimited number of plant functional types (PFTs). The current default setting of ORCHIDEE
138 distinguishes 15 PFTs where the meta-class of C3 grasslands have been separated into a boreal, temperate and
139 tropical C3 grassland PFT.

140

141 At the beginning of a simulation, each forest PFT in ORCHIDEE contains a monospecific forest stand that is
142 structured by a user-defined but fixed number of diameter classes (three by default). Throughout the simulation, the
143 boundaries of the diameter classes are adjusted to accommodate changes in the stand structure, while the number of
144 classes remains constant. Flexible class boundaries provide a computationally efficient approach to simulate
145 different forest structures. For instance, an even-aged forest is simulated by using a small diameter range between
146 the smallest and largest trees, resulting in all trees belonging to the same stratum. Conversely, an uneven-aged forest

147 is simulated by applying a wide range between diameter classes, such that different classes represent different
148 canopy strata.

149

150 The model uses allometric relationships to link tree height and crown diameter to stem diameter. Individual tree
151 canopies are not explicitly represented, instead a canopy structure model based on simple geometric forms (Haverd
152 et al. 2012) has been included in ORCHIDEE (Naudts et al., 2015). Diameter classes represent trees with different
153 mean diameter and height, which informs the user about the social position of trees within the canopy. Intra-stand
154 competition is based on the basal area of individual trees, which accounts for the fact that trees with a higher basal
155 area occupy dominant positions in the canopy and are therefore more likely to intercept light and thus contribute
156 more to stand-level photosynthesis and biomass growth compared to suppressed trees (Deleuze et al., 2004). If
157 recruitment occurs, diameter classes evolve into cohorts. However, in the absence of recruitment, all diameter classes
158 contain trees of the same age.

159

160 Individual tree mortality from self-thinning, wind storms, and forest management is explicitly simulated. Other
161 sources of mortality are implicitly accounted for through a so-called constant background mortality rate.
162 Furthermore, age classes (four by default) can be used after land cover change, forest management, and disturbance
163 events to explicitly simulate the regrowth of the forest. Following a land cover change, biomass and soil carbon
164 pools (but not soil water columns) are either merged or split to represent the various outcomes of a land cover
165 change. The ability of ORCHIDEE to simulate dynamic canopy structures (Chen et al., 2016; Naudts et al., 2015b;
166 Ryder et al., 2016), a feature essential to simulate both the biogeochemical and biophysical effects of natural and
167 anthropogenic disturbances, is exploited in other parts of the model, i.e., precipitation interception, transpiration,
168 energy budget calculations, the radiation scheme, and the calculation of the absorbed light for photosynthesis.

169

170 Since revision 7791, mortality from *Ips typographus* outbreaks is explicitly accounted for and thus conceptually
171 excluded from the so-called environmental background mortality. Subsequently, changes in canopy structure
172 resulting from growth, forest management, land cover changes, wind storms, and *Ips typographus* outbreaks are
173 accounted for in the calculations of the carbon, water, and energy exchanges between the land surface and the
174 atmosphere. For details on the functionality of the ORCHIDEE model that is not of direct relevance for this study,
175 e.g., energy budget calculations, soil hydrology, snow phenology, albedo, roughness, photosynthesis, respiration,
176 phenology, carbon and nitrogen allocation, land cover changes, product use, and the nitrogen cycle are readers are
177 referred to Krinner et al., 2005; Zaehle and Friend, 2010; Naudts et al., 2015; Vuichard et al., 2019.

178

179 2.2. **Origin of the bark beetle (*Ips typographus*) model: the LANDCLIM legacy**

180 Although mortality from windthrow (Yi-Ying et al., 2018) and forest management (Luyssaert et al., 2018; Naudts et
181 al., 2016) were already accounted for in ORCHIDEE prior to r8627, insect outbreaks and their interaction with other
182 disturbances were not. The LandClim model (Schumacher, 2004) and more specifically the *Ips typographus* model

183 developed by Temperli et al. (2013) has been used as basis to develop the *Ips typographus* model in ORCHIDEE
184 r8627.

185

186 LandClim is a spatially explicit stochastic landscape model in which forest dynamics are simulated at a yearly time
187 step for 10–100 km² landscapes consisting of 25 m × 25 m patches. Within a patch recruitment, growth, mortality
188 and competition among age cohorts of different tree species are simulated with a gap model (Bugmann, 1996) in
189 response to monthly mean temperature, climatic drought, and light availability. LandClim, for which a detailed
190 description can be found in (Schumacher, 2004; Temperli et al., 2013), includes the functionality to simulate the
191 decadal dynamics and consequences of *Ips typographus* outbreaks at the landscape-scale (Temperli et al., 2013). In
192 the LandClim approach, the extent, occurrence and severity of beetle-induced tree mortality are driven by the
193 landscape susceptibility, beetle pressure, and infested tree biomass. While the LandClim beetle model was designed
194 and structured to be generally applicable for northern hemisphere climate-sensitive bark beetle-host systems, it was
195 parameterized to represent disturbances by the *Ips typographus* in Norway spruce (*Picea abies* Karst.; Temperli et al.
196 2013).

197

198 As LandClim and ORCHIDEE are developed for different purposes, their temporal and spatial scales differ. These
199 differences in model resolution justify developing a new model while following the principles embedded in the
200 LandClim approach. LandClim assesses bark beetle damage at 25 m x 25 m patches and to do so it uses information
201 from other nearby patches as well as landscape characteristics such as slope, aspect and altitude. The susceptibility
202 of a landscape to bark beetle infestations is calculated using multiple factors such as drought-induced tree resistance,
203 age of the oldest spruce cohort, proportion of spruce in the patch's basal area, and spruce biomass damaged by
204 windthrow. These drivers are presented as sigmoidal relationships ranging from 0 to 1 (denoting none to maximum
205 susceptibility respectively) that are combined in a susceptibility index for each Norway spruce cohort in a patch.
206 Bark beetle pressure is quantified as the potential number of beetles that can infest a patch, and its calculation
207 considers, among others, previous beetle activity, maximum possible spruce biomass that beetles could kill, and
208 temperature-dependent bark beetle phenology. Finally, the susceptibility index and beetle pressure are used to
209 estimate the total infested tree biomass and total biomass killed by bark beetles for each cohort within a patch.

210

211 In ORCHIDEE, however, the simulation unit is about six orders of magnitude larger, i.e. 25 km x 25 km. Hence, a
212 single gridcell in ORCHIDEE exceeds the size of an entire landscape in LandClim. Where landscape characteristics
213 in LandClim can be represented by statistical distributions, the same characteristics in ORCHIDEE are represented
214 by single values. These differences between LandClim and ORCHIDEE imply that the original bark beetle model
215 cannot be implemented in ORCHIDEE without substantial adjustments; the model at the ORCHIDEE gridcell
216 should work without requiring spatial information and statistical distributions of landscape characteristics because
217 those are not available in ORCHIDEE.

218

219

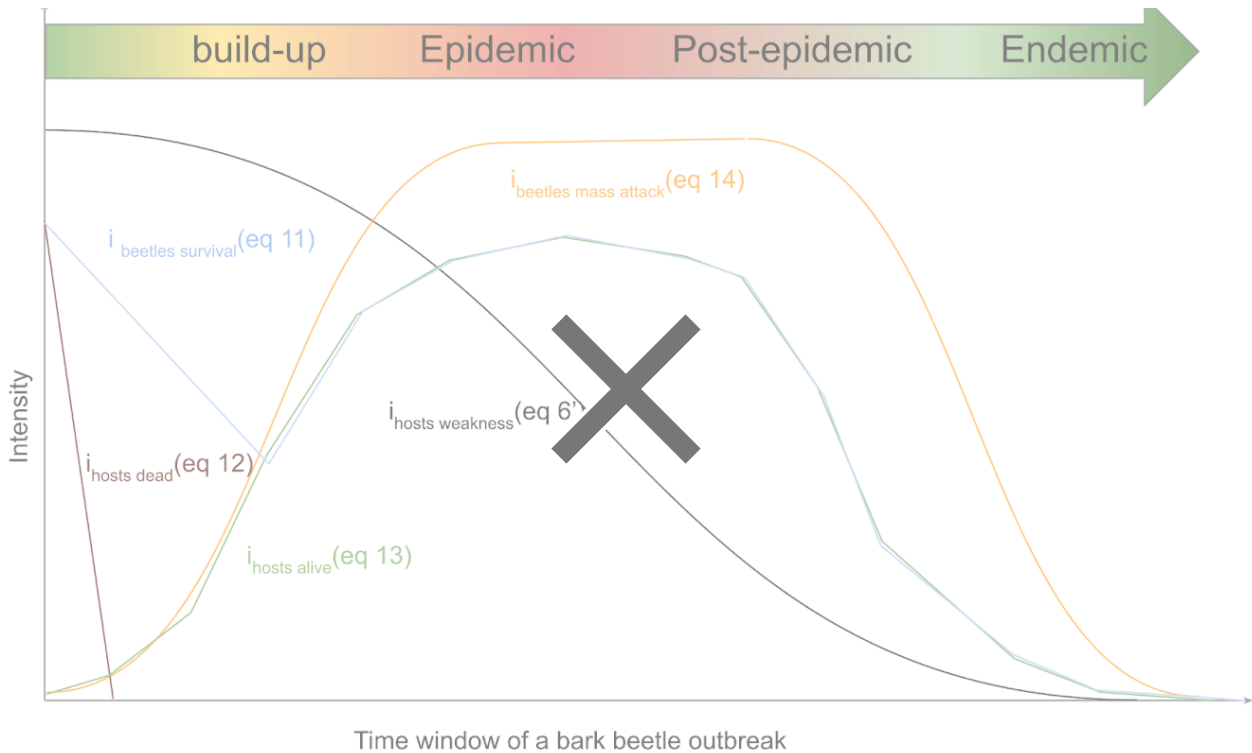


Figure 1 : Dynamic interplay of the different host and beetle characteristics during a bark beetle (*Ips typographus*) outbreak. The time window spans four outbreak development stages: build-up, epidemic, post-epidemic, and endemic. The curves represent key characteristics, showing the growth in beetle population and subsequent decline in host population. $i_{\text{hosts dead}}$ characterizes the presence of defenseless uprooted or cut spruce trees; $i_{\text{hosts alive}}$ characterizes living spruce trees that could become hosts for the bark beetles; $i_{\text{hosts susceptibility}}$ susceptibility of spruce trees to bark beetle attack; $i_{\text{beetles mass attack}}$ quantifies the capability of the bark beetles to mass attack; $i_{\text{beetles survival}}$ characterizes the survival of bark beetles. Host and bark beetle characteristics are detailed in the subsequent text. When the density of the host trees is declining due to an increased host mortality from the bark beetle outbreak itself, the competition between trees for light and nutrients declines as well. As a consequence, the host susceptibility decreases which in ORCHIDEE is the main pathway for an outbreak to move back to the endemic phase. After 1 year the wood from a storm is not fresh enough for bark beetles to breed in, so $i_{\text{host dead}}$ goes to zero. In ORCHIDEE, the bark beetle population needs to be capable of mass attacking living trees within a year to make the transition from the build-up to the epidemic phase.

220 2.3. Bark beetle outbreak development stages

221 Bark beetle outbreak development stages (Fig. 1) are useful to understand the dynamics of an outbreak (Edburg et
 222 al., 2012; Hlásny et al., 2021a; Wermelinger, 2004). Nonetheless, the outbreak model in ORCHIDEE r8627
 223 simulates the dynamic of the *Ips typographus* outbreak as a continuous process. Hence, endemic, epidemic, build-up
 224 and post-epidemic stages are not explicitly simulated. In this study, outbreak development stages were only
 225 introduced to structure the model description. If needed, these stages could be distinguished while post-processing
 226 the simulation results if (arbitrary) thresholds are set for specific variables such as DR_{beetles} .

227

Table 1: List of symbols

Symbol	Description	Units
α	Intercept of the self thinning relationship	unitless
β	Exponent of the self thinning relationship	unitless
$a_{ct,limit}$	B_{kill}/B_{total} at which $i_{beetles\ activity} = 0.5$	$gC.m^{-2}$
$B_{beetles\ kill}$	Biomass of spruce killed by bark beetle annually	$gC.m^{-2}$
$B_{windthrow\ kill}$	Biomass of spruce killed by windthrow event	$gC.m^{-2}$
$B_{beetles\ attacked}$	Biomass of spruce attacked by bark beetle annually	$gC.m^{-2}$
B_{total}	Total living biomass of spruce stand	$gC.m^{-2}$
B_{wood}	Woody biomass of spruce stand	$gC.m^{-2}$
BP_{limit}	$i_{beetle\ pressure}$ at which $i_{beetles\ mass\ attack} = 0.5$	unitless
D_{max}	Maximum stand density	$tree.ha^{-1}$
$D_{age\ class}$	Stand tree density of spruce age classes	$tree.ha^{-1}$
D_{spruce}	Stand tree density of spruce	$tree.ha^{-1}$
DD_{eff}	Cumulative effective degrees days	$^{\circ}C.Day^{-1}$
DD_{ref}	Reference degrees days to complete one beetle generation	$^{\circ}C.Day^{-1}$
$Dia_{quadratic}$	Mean quadratic diameter	meters
$DR_{beetles}$	$B_{beetles\ kill}/B_{total} * 100$	%
$DR_{windthrow}$	$B_{windthrow\ kill}/B_{total} * 100$	%
F_{spruce}	Area fraction of spruce within gridcell	unitless
$F_{age\ class}$	Area fraction of spruce age classes	unitless
$F_{non-spruce}$	Non-spruce area fraction	unitless
G_{limit}	Beetles generation number at which $i_{beetle\ generation} = 0.5$	Generation
$I_{hosts\ competition}$	Spruce trees under competition pressure	unitless
$I_{hosts\ susceptibility}$	Spruce trees susceptibility to bark beetle attack	unitless
$I_{hosts\ attractivity}$	Spruce attractivity for bark beetles	unitless
$I_{hosts\ dead}$	Defenseless spruce trees uprooted or cut	unitless
$I_{hosts\ alive}$	Potential living hosts for bark beetle	unitless
$I_{hosts\ defense}$	Spruce trees capability to resist a bark beetle attack	unitless
$I_{hosts\ share}$	Spruces hidden by other species to bark beetle detection	unitless
$I_{hosts\ competition, age\ class}$	Spruce age class under competition pressure	unitless
$I_{hosts\ defense, age\ class}$	Spruce age class capability to resist a bark beetle attack	unitless
$I_{hosts\ health, age\ class}$	Spruce age class health condition	unitless
$I_{beetles\ pressure}$	Proxy of bark beetle population level	unitless
$I_{beetles\ survival}$	Bark beetle survival index	unitless
$I_{beetles\ generation}$	Bark beetle generation index	unitless

$i_{\text{beetles_activity}}$	Previous bark beetles activity index	unitless
$i_{\text{beetles_mass_attack}}$	Bark beetles mass attack capability	unitless
$\text{max}_{N_{\text{wood}}}$	Value of N_{wood} at which $i_{\text{hosts dead}} = 1.0$	unitless
N_{wood}	Spruce woody necromass	gC.m^{-2}
$P_{\text{success, age_class}}$	Probability of successful attack per age class	unitless
P_{attack}	Probability of beetles attack	unitless
PWS_{max}	Maximum long term spruce water stress	unitless
PWS_{spruce}	Spruce water stress	unitless
$PWS_{\text{age_class}}$	Spruce age classes water stress	unitless
PWS_{limit}	Spruce water stress at which $i_{\text{hosts defense}} = 0.5$	unitless
$i_{\text{rd_limit}}$	Relative density index at which $i_{\text{hosts competition}} = 0.5$	unitless
$i_{\text{rd_susceptibility}}$	Relative density index at which $i_{\text{host susceptibility}} = 0.5$	unitless
$i_{\text{rd_spruce}}$	Spruce stand relative density index [0,1]	unitless
$I_{\text{rd, age class}}$	Spruce age classes relative density index [0,1]	unitless
$S_{\text{competition}}$	Shape parameter in the calculation of $i_{\text{hosts competition}}$	unitless
$S_{\text{susceptibility}}$	Shape parameter in the calculation of $i_{\text{hosts susceptibility}}$	unitless
S_{arought}	Shape parameter in the calculation of $i_{\text{hosts defense}}$	unitless
S_{share}	Shape parameter in the calculation of $i_{\text{hosts share}}$	unitless
S_{activity}	Shape parameter in the calculation of $i_{\text{beetle activity, y-1}}$	unitless
$S_{\text{generation}}$	Shape parameter in the calculation of $i_{\text{beetle generation}}$	unitless
Sh_{spruce}	Share fraction of spruce against non-spruce in gridcell	unitless
Sh_{limit}	Share fraction at which $i_{\text{hosts share}} = 0.5$	unitless
T_{air}	Air temperature	$^{\circ}\text{C}$
T_{max}	Temperature above which beetles developpement stop	$^{\circ}\text{C}$
T_{min}	Temperature below which beetles developpement stop	$^{\circ}\text{C}$
T_{bark}	Bark temperature	$^{\circ}\text{C}$
T_{opt}	Optimal bark temperature for beetles development	$^{\circ}\text{C}$

Table 1: List of symbols

Symbol	Description	Units
α	Intercept of the self thinning relationship	unitless
β	Exponent of the self thinning relationship	unitless
a	Underscore a represent a age class	unitless
act_{limit}	$B_{\text{kill}}/B_{\text{total}}$ at which $i_{\text{beetles activity}} = 0.5$	gC.m^{-2}
$B_{\text{beetles kill}}$	Biomass of spruce killed by bark beetle annually	gC.m^{-2}
$B_{\text{windthrow kill}}$	Biomass of spruce killed by windthrow event	gC.m^{-2}

$B_{\text{beetles attacked}}$	Biomass of spruce attacked by bark beetle annually	gC.m^{-2}
B_{total}	Total living biomass of spruce stand	gC.m^{-2}
B_{wood}	Woody biomass of spruce stand	gC.m^{-2}
BP_{limit}	$i_{\text{beetle pressure}}$ at which $i_{\text{beetles mass attack}} = 0.5$	unitless
D_{max}	Maximum stand density	tree.ha^{-1}
$D_{\text{spruce, a}}$	Stand tree density of spruce age classes	tree.ha^{-1}
D_{spruce}	Stand tree density of spruce	tree.ha^{-1}
DD_{eff}	Cumulative effective degrees days	$^{\circ}\text{C.Day}^{-1}$
DD_{ref}	Reference degrees days to complete one beetle generation	$^{\circ}\text{C.Day}^{-1}$
$Dia_{\text{quadratic}}$	Mean quadratic diameter	meters
DR_{beetles}	$B_{\text{beetles kill}}/B_{\text{total}} * 100$	%
$DR_{\text{windthrow}}$	$B_{\text{windthrow kill}}/B_{\text{total}} * 100$	%
F_{spruce}	Area fraction of spruce within gridcell	unitless
$F_{\text{spruce, a}}$	Area fraction of spruce age classes	unitless
$F_{\text{non-spruce}}$	Non-spruce area fraction	unitless
G_{limit}	Beetles generation number at which $i_{\text{beetle generation}} = 0.5$	Generation
$i_{\text{hosts competition}}$	Spruce trees under competition pressure	unitless
$i_{\text{hosts susceptibility}}$	Spruce trees susceptibility to bark beetle attack	unitless
$i_{\text{hosts attractivity}}$	Spruce attractivity for bark beetles	unitless
$i_{\text{hosts dead}}$	Defenseless spruce trees uprooted or cut	unitless
$i_{\text{hosts alive}}$	Potential living hosts for bark beetle	unitless
$i_{\text{hosts defense}}$	Spruce trees capability to resist a bark beetle attack	unitless
$i_{\text{hosts share}}$	Spruces hidden by other species to bark beetle detection	unitless
$i_{\text{hosts competition, a}}$	Spruce age class under competition pressure	unitless
$i_{\text{hosts defense, a}}$	Spruce age class capability to resist a bark beetle attack	unitless
$i_{\text{hosts health, a}}$	Spruce age class health condition susceptibility	unitless
$i_{\text{beetles pressure}}$	Proxy of bark beetle population level	unitless
$i_{\text{beetles survival}}$	Bark beetle survival index	unitless
$i_{\text{beetles generation}}$	Bark beetle generation index	unitless
$i_{\text{beetles_activity}}$	Previous bark beetles activity index	unitless
$i_{\text{beetles_mass_attack}}$	Bark beetles mass attack capability	unitless
$i_{\text{rd limit}}$	Relative density index at which $i_{\text{hosts competition}} = 0.5$	unitless
$i_{\text{rd susceptibility}}$	Relative density index at which $i_{\text{host susceptibility}} = 0.5$	unitless
$i_{\text{rd spruce}}$	Spruce stand relative density index [0,1]	unitless
$i_{\text{rd spruce, a}}$	Spruce age classes relative density index [0,1]	unitless
$max_{N_{\text{wood}}}$	Value of N_{wood} at which $i_{\text{hosts dead}} = 1.0$	unitless
N_{wood}	Spruce woody necromass	gC.m^{-2}

$P_{success, a}$	Probability of successful attack per age class	unitless
P_{attack}	Probability of beetles attack	unitless
PWS_{max}	Maximum long term spruce water stress	unitless
$PWS_{y, spruce}$	Spruce water stress	unitless
$PWS_{y, spruce, a}$	Spruce age classes water stress	unitless
PWS_{limit}	Spruce water stress at which $i_{hosts\ defense} = 0.5$	unitless
$S_{competition}$	Shape parameter in the calculation of $i_{hosts\ competition}$	unitless
$S_{susceptibility}$	Shape parameter in the calculation of $i_{hosts\ susceptibility}$	unitless
$S_{drought}$	Shape parameter in the calculation of $i_{hosts\ defense}$	unitless
S_{share}	Shape parameter in the calculation of $i_{hosts\ share}$	unitless
$S_{activity}$	Shape parameter in the calculation of $i_{beetle\ activity, y-1}$	unitless
$S_{generation}$	Shape parameter in the calculation of $i_{beetle\ generation}$	unitless
Sh_{spruce}	Share fraction of spruce against non-spruce in gridcell	unitless
Sh_{limit}	Share fraction at which $i_{hosts\ share} = 0.5$	unitless
T_{air}	Air temperature	°C
T_{max}	Temperature above which beetles development stop	°C
T_{min}	Temperature below which beetles development stop	°C
T_{bark}	Bark temperature	°C
T_{opt}	Optimal bark temperature for beetles development	°C

230

231 The biomass of trees killed by bark beetles in one year and one gridcell ($B_{beetles\ kill}$) is calculated as the product of the
 232 biomass of trees attacked by bark beetles ($B_{beetles\ attacked}$) and the probability of a successful attack ($P_{success, \text{age class } a}$)
 233 averaged over the number of spruce age classes and weighted by their actual fraction ($F_{age\ class} F_{spruce, a} / F_{spruce}$). The
 234 approach assumes that a successful beetle colonization always results in the death of the attacked tree which is a
 235 simplification from reality (A. Leufvén et al. 1986).

236

$$\begin{aligned}
 237 \quad B_{beetles\ kill} &= \sum_{\text{nb age classes}}^{age\ class=1} P_{success, \text{age class}} \times B_{beetles\ attacked} \times \frac{F_{age\ class}}{F_{spruce}} \\
 238 \quad B_{beetles\ kill} &= \sum_{a=1}^3 P_{success, a} \times B_{beetles\ attacked} \times \frac{F_{spruce, a}}{F_{spruce}} \quad (1)
 \end{aligned}$$

239

240 During the endemic stage, $B_{beetles\ attacked}$ and $B_{beetles\ kill}$ are at their lowest values and the damage from bark beetles has
 241 little impact on the structure and function of the forest. Losses from $B_{beetles\ kill}$ can be considered to contribute to the
 242 background mortality.

243

244 The biomass of trees attacked by bark beetles ($B_{beetles\ attacked}$) is the outcome of bark beetles that successfully overcame
 245 the tree defenses and succeeded in boring holes in the bark in order to reach the sapwood. $B_{beetles\ attacked}$ is calculated at

246 the gridcell by multiplying the actual stand biomass of spruce (B_{total}) and the probability that bark beetles attack
 247 spruce trees in the gridcell ($P_{attacked}$).

248

$$249 \quad B_{\text{beetles attacked}} = B_{\text{total}} \times P_{\text{attacked}} \quad B_{\text{beetles attacked}} = B_{\text{total}} \times P_{\text{attacked}}$$

250 (2)

251

252 $P_{attacked}$ represent the ability of the bark beetles to spread and to locate new suitable spruce trees as hosts for breeding.

253 $P_{attacked}$ is calculated by the product of two indexes (all indexes in this study are denoted i and are analogue the

254 susceptibility indexes from Temperli et al. 2013): (1) the beetle pressure index ($i_{\text{beetles pressure}}$) which a proxy of the bark

255 beetle population and (2) the stand attractivity index ($i_{\text{hosts attractivity}}$) is related to its health and reflects the ability of the

256 forest to resist an external stressor such as bark beetle attacks.

257

$$258 \quad P_{\text{attacked}} = i_{\text{hosts attractivity}} \times i_{\text{beetles pressure}} \quad P_{\text{attacked}} = i_{\text{hosts attractivity}} \times i_{\text{beetles pressure}}$$

259 (3)

260

261 2.6. Host attractivity

262 The stand attractivity index ($i_{\text{hosts attractivity}}$) represents how interesting a stand is for a new bark beetle colony. When

263 $i_{\text{hosts attractivity}}$ tends to 0, the stand is constituted mainly by healthy trees which are less attractive for beetles whereas an

264 $i_{\text{hosts attractivity}}$ approaching 1 represents a highly stressed spruce stand suitable for colonization by bark beetles. Factors

265 that contribute to the stress of a forest are: nitrogen limitation, limited carbohydrate reserves, and monospecific

266 spruce forest. Trees experiencing extended periods of environmental stress are expected to have less carbon and

267 nitrogen reserves available for defense compounds, making them vulnerable for bark beetle attacks even at relatively

268 low beetle population densities (Raffa et al., 2008). Nonetheless, reserves pools in ORCHIDEE r8627 have not yet

269 been evaluated so, instead proxies were used such as long term drought (PWS_{max}) and relative density index ($i_{rd, spruce}$)

270 which were already simulated in ORCHIDEE r8627.

271

$$272 \quad i_{\text{hosts attractivity}} = \max(i_{\text{hosts competition}}, i_{\text{hosts defense}}) \times i_{\text{hosts share}} \quad (4)$$

273

274 Where $i_{\text{hosts competition}}$ and $i_{\text{hosts defense}}$ both represent proxies for the reduction of the nitrogen and carbohydrate reserve due

275 to strong competition for light and soil resources, and consecutive years that are drier than average. For this study,

276 the maximum drought intensity during the last three years (PWS_{max}) is considered, as a proxy of spruce stand

277 healthiness:

278

$$279 \quad i_{\text{hosts defense}} = 1 / (1 + e^{S_{\text{drought}} \cdot (1 - PWS_{\text{max}} - PWS_{\text{limit}})}) \quad i_{\text{hosts defense}} = 1 / (1 + e^{S_{\text{drought}} \cdot (1 - PWS_{\text{max}} - PWS_{\text{limit}})})$$

280 (5a)

281

$$\begin{aligned}
282 \quad PWS_{max} &= \sum_{nb \text{ age class}=3}^{age \text{ class}=1} \max(PWS_{spruce, n}, PWS_{spruce, n-1}, PWS_{spruce, n-2}) \\
283 \quad PWS_{max} &= \sum_{a=1}^3 \max(PWS_y, PWS_{y-1}, PWS_{y-2}) \times \frac{F_{spruce \text{ class}}}{F_{spruce}} \times \frac{F_{spruce, a}}{F_{spruce}} \quad (5b)
\end{aligned}$$

284

285 Where PWS_{spruce} is the average daily plant water stress index over the growing season for the spruce stand
286 and is equal to 0 when plants are highly stressed and equal to 1 when plants are not stressed. PWS_{limit} is the plant
287 water stress below which the healthiness of the stand will strongly be affected. $Nb \text{ age class}$ is the numbers age class
288 within the stand and is equal to 3 in this study. In addition to drought, overstocked forest may also decrease the
289 overall healthiness of a spruce stand ($i_{hosts \text{ competition}}$).

290

$$\begin{aligned}
291 \quad i_{hosts \text{ competition}} &= 1 / (1 + e^{S_{competition} \cdot (i_{rd \text{ spruce}} - i_{rd \text{ limit}})}) \\
292 \quad i_{hosts \text{ competition}} &= 1 / (1 + e^{S_{competition} \cdot (i_{rd \text{ spruce}} - i_{rd \text{ limit}})}) \quad (6a)
\end{aligned}$$

293

294 In ORCHIDEE, the relative density index (i_{rd}) is used to quantify the competition between trees at the stand level. At
295 an i_{rd} of 1, the forest is expected to be at its maximum density given the carrying capacity of the site, implying the
296 highest level of competition between trees. $i_{rd \text{ limit}}$ represents the limit at which the bark beetle outbreak starts to
297 decline because of lack of suitable host trees. The severity of bark beetle-caused tree mortality decreases when we
298 increase the spatial resolution from the stand to the landscape scale. At the landscape scale, which can cover areas up
299 to 2500 km², the duration of mortality may be longer and the severity lower because beetles disperse across the
300 landscape and cause mortality at different times. This distinction is important for interpreting model results,
301 particularly when considering parameters like $i_{rd \text{ limit}}$ in the ORCHIDEE model. $i_{rd \text{ limit}}$ describes the proportion of trees
302 surviving after an outbreak and should therefore be adjusted for the spatial scale of a gridcell in ORCHIDEE. In
303 model set-up where a gridcell represents a single stand (~1 ha), $i_{rd \text{ limit}}$ should be close to 0, indicating that nearly all
304 trees may be killed. However, in a simulation with gridcells representing 2500 km², not all trees will be killed, which
305 is reflected in setting $i_{rd \text{ limit}}$ to 0.4.

306

307 $i_{rd \text{ spruce}}$ is computed as follows:

308

$$309 \quad i_{rd \text{ spruce}} = \sum_{nb \text{ age class}=3}^{age \text{ class}=1} \frac{D_{age \text{ class}}}{D_{max}} \times \frac{F_{age \text{ class}}}{F_{spruce}} \times \frac{D_{spruce, a}}{D_{max}} \times \frac{F_{spruce, a}}{F_{spruce}} \quad (6b)$$

310

311 Where $D_{age \text{ class}}$ is the current tree density of an age class and $F_{age \text{ class}}$ is the fraction of spruce in the
312 gridcell that resides in this age class. D_{max} represents the maximum stand density of a stand given its diameter. In
313 ORCHIDEE D_{max} is calculated based on the quadratic mean diameter (cm) of the age class and two species specific
314 parameters, α and β :

315

$$316 \quad D_{max} = (Dia_{quadratic, age class} / \alpha)^{(1/\beta)} D_{max} = (Dia_{quadratic} / \alpha)^{(1/\beta)}$$

317 (6c)

318

319 The index $i_{hosts share}$ (used in eq. 4) takes into account that in a mixed tree species landscape, even a few non-host trees
 320 may chemically hinder bark beetles in finding their host trees (Zhang and Schlyter, 2004) explaining why insect
 321 pests, including *Ips typographus* outbreaks, often cause more damage in pure compared to mixed stands (Nardi et al.,
 322 2023). ORCHIDEE r8627 does not simulate multi-species stands but does account for landscape-level heterogeneity
 323 of forests with different plant functional types. The bark beetle model in ORCHIDEE assumes that within a gridcell,
 324 the fraction of spruce over other tree species is a proxy for the degree of mixture:

325

$$326 \quad i_{hosts share} = 1 / (1 + e^{S_{share} \cdot (SH_{spruce} - SH_{limit})}) \quad (7a)$$

327

328 Where,

329

$$330 \quad Sh_{spruce} = \frac{F_{non-spruce}}{F_{spruce}} Sh_{spruce} = F_{non-spruce} / F_{spruce}$$

331 (7b)

332

333 2.7. Implicit representation of bark beetle populations

334 The bark beetle pressure Index ($i_{beetles pressure}$) is now formulated based on two components: (1) the bark beetle
 335 breeding index of the current year ($i_{beetles generation}$), and (2) an index of the loss of tree biomass in the previous year due
 336 to bark beetle infestation ($i_{beetles activity}$). $i_{beetles activity}$ is thus a proxy of the previous year's bark beetle activity. The
 337 expression accounts for the legacy effect of bark beetle activities by averaging activities over the current and
 338 previous years. In this approach, the susceptibility index ($i_{beetles survival}$) serves as an indicator for increased bark beetle
 339 survival which could result from favorable conditions for beetle demography (see next section).

340

$$341 \quad i_{beetles pressure} = i_{beetles survival} \times \frac{(i_{beetles generation} + i_{beetles activity})}{2}$$

$$342 \quad i_{beetles pressure} = i_{beetles survival} \times \frac{(i_{beetles generation} + i_{beetles activity})}{2} \quad (8)$$

343

344 The model calculates $i_{beetles generation}$ from a logistic function, which depends on the number of generations a bark beetle
 345 population can sustain within a single year:

346

$$347 \quad i_{beetles generation} = 1 / (1 + e^{-S_{generation} \cdot (\frac{DD_{eff}}{DD_{ref}} - G_{limit})}) i_{beetles generation} = 1 / (1 + e^{-S_{generation} \cdot (\frac{DD_{eff}}{DD_{ref}} - G_{limit})})$$

348 (9)

349 Where $S_{generation}$ and G_{limit} are tuning parameters for the logistic function, DD_{eff} represents the sum of effective
 350 temperature for bark beetle reproduction in $^{\circ}\text{C}\cdot\text{Day}^{-1}$, while DD_{ref} denotes the thermal sum of degree days for one
 351 bark beetle generation in $^{\circ}\text{C}\cdot\text{Day}^{-1}$. Saturation of $i_{beetles\ generation}$ represents the lack of available breeding substrate
 352 when many generations develop over a short period.

353

354 DD_{eff} is calculated from January 1st until the diapause of the first generation. In ORCHIDEE, diapause is triggered
 355 when daylength exceeds 14.5 hours (e.g., April 27th for France). Each day before the diapause with a daily average
 356 temperature around the bark above 8.3°C (T_{min}) and below 38.4°C (T_{max}) is accounted for in the summation of DD_{eff}
 357 (eq.10). This approach simulates the phenology of bark beetles, which tend to breed earlier when winter and spring
 358 were warmer, thus allowing for multiple generations in the same year (Hlásny et al., 2021a).

$$359 \quad DD_{eff} = \sum_{n_{diapause}}^{i=1} (T_{opt} - T_{min}) * e^{(0.0288 * T_{bark,i})} - e^{(0.0288 * b_{eff} - (40.99 - T_{bark,i})/3.59)} - 1.25$$

$$360 \quad DD_{eff} = \sum_{n_{diapause}}^{i=1} (T_{opt} - T_{min}) * e^{(0.0288 * T_{bark,i})} - e^{(0.0288 * b_{eff} - (40.99 - T_{bark,i})/3.59)} - 1.25 \quad (10)$$

361

362 Where i is a day, $n_{diapause}$ is the number of days between the 1st of January and the day of the diapause. T_{opt} (30.3°C) is
 363 the optimal bark temperature for ~~beetles~~ beetle development and T_{min} (8.3°C) is the temperature below which the
 364 beetles ~~developement stop~~ development stops. $T_{bark,i}$ is the average daily bark temperature. $T_{bark,i}$ is calculated as the
 365 daily average air temperature minus 2°C . All parameters values are taken from Temperli et al. 2013

366 The bark beetle activity of the previous year ($i_{beetles\ activity}$) is calculated as:

367

$$368 \quad i_{beetles\ activity} = 1 / (1 + e^{-S_{activity} * (\frac{B_{kill,y-1}}{B_{total}} - act_{limit})}) \quad (11)$$

369

370 Where $i_{beetles\ activity}$ denotes the biomass of the stand damaged by bark beetles in the previous year, B_{total} is the total
 371 biomass of the stand, and $S_{activity}$ and act_{limit} are parameters that drive the intensity of this negative feedback.

372

373 During the build-up stage the population of bark beetles can either return to its endemic stage if tree defense
 374 mechanisms are preventing bark beetles from successfully attacking healthy trees, or evolve into an epidemic stage
 375 (Fig. 1) if the tree defense mechanisms fail. During the post-epidemic stage, the forest is still subject to higher
 376 mortality than usual but signs of recovery appear (Hlásny et al., 2021a). Recovery may help the forest ecosystem to
 377 return to its original state or switch to a new state (different species, change in the forest structure) depending on the
 378 intensity and the frequency of the disturbance (Van Meerbeek et al., 2021).

379

380 2.8. Bark beetle survival

381 The capability of the bark beetles to survive the winter in between two breeding seasons is critical in simulating
 382 epidemic outbreaks. During regular winters, winter mortality for bark beetles is around 40% for the adults and 100%

383 for the juveniles (Jönsson et al. 2012). In our scheme, this mortality rate is implicitly accounted for in the calculation
 384 of the bark beetle survival index ($i_{beetles\ survival}$). A lack of data linking bark beetle survival to anomalous winter
 385 temperatures, justifies the implicit approach and prevented including this information as a modulator of $i_{beetles\ survival}$.
 386 The latter explains why winter temperatures do not appear in eq. 11. Instead the model simulates the survival as a
 387 function of the abundance of suitable tree hosts which decreases the competition for shelter and food:

388

$$389\ i_{beetles\ survival} = \max(i_{hosts\ dead}, i_{hosts\ alive}) \quad (12)$$

390

391 The availability of wood necromass from trees that died recently, particularly following windstorms, plays a critical
 392 role in bark beetle survival and proliferation. In the year following a windstorm, uprooted and broken trees may offer
 393 an ideal breeding substrate for bark beetles, facilitating their population growth.

394

395 In Temperli et al. (2013) an empirical correlation between windthrow events and bark beetle susceptibility was
 396 established. ORCHIDEE enhances realism by considering the actual suitable hosts (living or recently dead trees) as
 397 the primary driver of bark beetle survival. To avoid overestimating bark beetle population growth, $max_{N_{wood}}$ has been
 398 introduced. Any addition of dead trees beyond $max_{N_{wood}}$ is considered ineffective in affecting the bark beetle
 399 population. This ensures that an excess of breeding substrate does not artificially inflate beetle numbers.

400 This relationship is quantitatively represented in ORCHIDEE through the dead host index, $i_{hosts\ dead}$, which is driven
 401 by the availability of recent dead trees. The formulation of $i_{hosts\ dead}$ is as follows:

402

$$403\ i_{hosts\ dead} = \min\left(\frac{N_{wood}}{B_{wood}} / \max_{N_{wood}}, 1\right) i_{hosts\ dead} = \min\left(\frac{N_{wood}}{B_{wood}} / \max_{N_{wood}}, 1\right)$$

404 (13)

405

406 Here, N_{wood} represents the quantity of woody necromass from the current year, B_{wood} is the total living woody biomass
 407 in the stand, and $max_{N_{wood}}$ is the threshold of the ratio N_{wood}/B_{wood} signifying the maximum level. This index captures
 408 the immediate increase in dead trees suitable for bark beetle breeding following a windthrow event. However, it
 409 takes about a year for dead wood to lose its freshness and suitability for bark beetle breeding. This is accounted for
 410 by excluding woody necromass that is older than 1 year from the $i_{hosts\ dead}$ calculation.

411

412 $max_{N_{wood}}$ can also be considered as a parameter that depends on the spatial scale of the simulation. The mortality rate
 413 of trees ($DR_{windthrow}$) that will trigger an outbreak is very different across spatial scales. Where a relatively high share
 414 of dead wood is needed to trigger an outbreak at the patch-scale, a much lower share of dead wood suffices at the
 415 landscape-scale to trigger a widespread bark beetle outbreak. So these parameters must be set according to the spatial
 416 resolution of the simulation experiment.

417

418 $i_{hosts\ alive}$ denotes the survival of bark beetles which is facilitated by the abundance of suitable trees which reduces the
 419 competition among bark beetles for breeding substrates and therefore increases their survival.

420

$$421 \ i_{hosts\ alive} = i_{beetles\ mass\ attack} \times i_{hosts\ susceptibility} \ i_{hosts\ alive} = i_{beetles\ mass\ attack} \times i_{hosts\ susceptibility}$$

$$422 \quad (14)$$

423

424 The amount of suitable tree hosts $i_{hosts\ alive}$ is driven by two factors: (1) the abundance of weak trees which can be
 425 more easily infected by bark beetles. ORCHIDEE does not explicitly represent weak trees, but tree health is thought
 426 to decrease with an increasing density given the stand diameter. The index for host suitability is thus calculated by
 427 making use of the relative density index ($i_{rd\ spruce}$).

428

$$429 \ i_{hosts\ susceptibility} = 1 / (1 + e^{S_{susceptibility} \cdot (i_{rd\ spruce} - i_{rd\ susceptibility})})$$

$$430 \ i_{hosts\ susceptibility} = 1 / (1 + e^{S_{susceptibility} \cdot (i_{rd\ spruce} - i_{rd\ susceptibility})}) \quad (6a')$$

431

432 Equation 6a' is close to equation 6a but the parameter $S_{susceptibility}$ has been reduced by a factor of two in order to
 433 reflect that $i_{hosts\ susceptibility}$ is more sensitive to $i_{rd\ spruce}$ than $i_{hosts\ competition}$. (2) $i_{hosts\ mass\ attack}$ which represent the ability of
 434 bark beetles to attack healthy trees when the number of bark beetles is large enough. This index only depends on the
 435 size of the bark beetle population ($i_{beetles\ pressure}$ see eq. 8)

436

$$437 \ i_{hosts\ mass\ attack} = 1 / (1 + e^{S_{mass\ attack} \cdot (i_{beetles\ pressure} - BP_{limit})})$$

$$438 \ i_{hosts\ mass\ attack} = 1 / (1 + e^{S_{mass\ attack} \cdot (i_{beetles\ pressure} - BP_{limit})}) \quad (15)$$

439

440 Where $S_{hosts\ mass\ attack}$ and BP_{limit} are parameters. $S_{mass\ attack}$ controls the steepness of the relationship while BP_{limit} is the
 441 bark beetle pressure index at which the population is moving from endemic to epidemic stage where mass attacks are
 442 possible.

443

444 The epidemic stage corresponds to the capability of bark beetles to mass attack healthy trees and overrule tree
 445 defenses (Biedermann et al., 2019). At this point in the outbreak, all trees are potential targets irrespective of their
 446 health. Three causes have been suggested to explain the end of the epidemic phase: (1) the most likely cause is a
 447 high interspecific competition among beetles for tree host when the density is decreasing (decreasing $i_{hosts\ alive}$)
 448 (Komonen et al., 2011; Pineau et al., 2017), (2) a series of very cold years will decrease their ability to reproduce
 449 (decreasing $i_{beetles\ generation}$), and (3) a rarely demonstrated increasing population of beetle predators (Berryman, 2002).
 450 In ORCHIDEE r8627, the first two causes are represented but the last, i.e. the predators are not.

451

452 2.9. Tree mortality from bark beetle infestation

453 When bark beetles attack a tree, the success of their attack will likely depend on the capability of the tree to defend
 454 itself from the attack. Trees defend themselves against beetle attacks by producing secondary metabolites (Huang et
 455 al., 2020). The high carbon and nitrogen costs of these compounds limit their production to periods with
 456 environmental conditions favorable for growth (Lieutier, 2002). The probability of a successful bark beetle attack is
 457 driven by the size of the bark beetle population ($i_{beetles\ pressure}$) and the health of each tree. ORCHIDEE, however, is not
 458 simulating individual trees but rather diameter classes within an age class. An index of tree health for each age class
 459 ($i_{hosts\ health,\ age\ class\ a}$) was calculated as:

460

$$461 \quad P_{success,\ age\ class} = i_{hosts\ health,\ age\ class} \times i_{beetles\ pressure} \quad P_{success,\ a} = i_{hosts\ health,\ a} \times i_{beetles\ pressure}$$

462 (16)

463

464 A tree rarely dies solely from bark beetle damage (except during mass attacks) as female beetles often carry
 465 blue-stain fungi, which colonizes the phloem and sapwood, blocking the water-conducting vessels of the tree
 466 (Ballard et al., 1982). This results in tree death from carbon starvation or desiccation. As ORCHIDEE r8627 does
 467 not simulate the effects of changes in sapwood conductivity on photosynthesis and the resultant probability of tree
 468 mortality, the index of weakened trees $i_{hosts\ health,\ age\ class\ a}$ makes use of two proxies similarly to equation 5 and 6
 469 but simplified to be calculated only for one age class at a time:

470

$$471 \quad i_{hosts\ health,\ age\ class} = \frac{(i_{hosts\ competition,\ age\ class} + i_{hosts\ defense,\ age\ class})}{2} \quad i_{hosts\ health,\ a} = \frac{(i_{hosts\ competition,\ a} + i_{hosts\ defense,\ a})}{2}$$

472 (17)

473

$$474 \quad i_{hosts\ defense,\ age\ class} = 1 / (1 + e^{S_{drought} \cdot (1 - PWS_{age\ class} - PWS_{limit})})$$

$$475 \quad i_{hosts\ defense,\ a} = 1 / (1 + e^{S_{drought} \cdot (1 - PWS_{y,\ spruce,\ a} - PWS_{limit})}) \quad (5a')$$

476

477 Contrary to equation 5a, $PWS_{age\ class}$ PWS_a is the plant water stress from the current year.

478

$$479 \quad i_{hosts\ competition,\ age\ class} = 1 / (1 + e^{S_{competition} \cdot (i_{rd\ age\ class} - i_{rd\ limit})})$$

$$480 \quad i_{hosts\ competition,\ a} = 1 / (1 + e^{S_{competition} \cdot (i_{rd\ spruce,\ a} - i_{rd\ limit})}) \quad (6a'')$$

481

$$482 \quad i_{rd\ age\ class} \cdot i_{rd\ spruce,\ a} = \frac{D_{age\ class}}{D_{max}} \cdot \frac{D_{spruce,\ a}}{D_{max}} \quad (6b'')$$

483

484 To assess the bark beetle damage rate ($DR_{beetles}$), $B_{beetles\ kill}$ has to be divided by B_{total} .

485

486 **2.10. Flow of the calculations**

487 The equations presented above contain feedback loops which have been visualized in Fig. 2. In ORCHIDEE these
 488 feedback loops are accounted for in subsequent time steps rather than the same time step.
 489

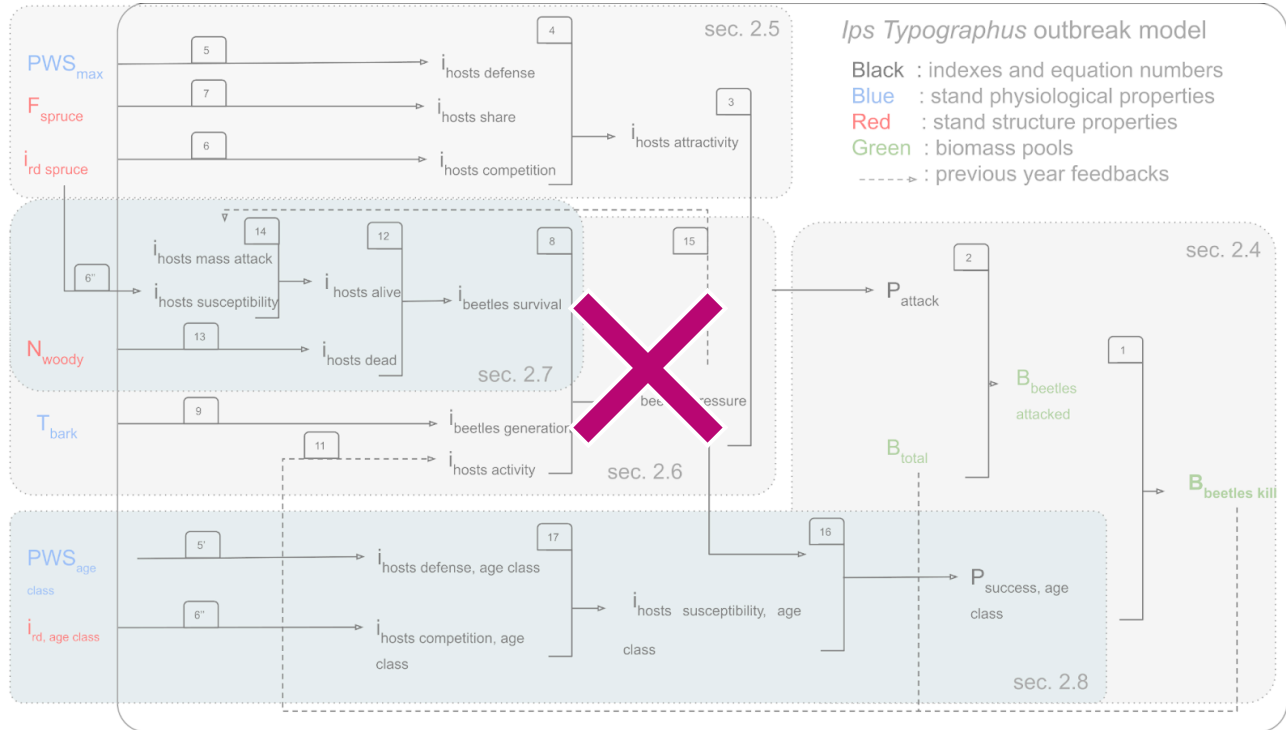


Figure 2: Order of the calculations and feedback in the *Ips typographus* outbreak model of ORCHIDEE. The numbers correspond to the equation numbers in this study. The dotted line boxes represent 5 main concepts of the outbreak model described in section 2.4, 2.5, 2.6, 2.7, 2.8. The variable name definitions are listed in table 1.

490

491 **3. Methods and material**

492 **3.1. Model configuration**

493 Given the large-scale nature of the ORCHIDEE, a sensitivity experiment of the bark beetle outbreak functionality
 494 was carried out rather than focusing the model evaluation on matching observed damage volumes at specific case
 495 studies. Focussing on model sensitivity for a range of environmental conditions is thought to reduce the risk of
 496 overfitting the model to specific site conditions (Abramowitz et al., 2008).

497

498 ORCHIDEE r8627 including the bark beetle model was run at the location of eight FLUXNET sites, selected to
 499 simulate a credible temperature and precipitation gradient for spruce (see below). For each location, the half-hourly
 500 meteorological data from the flux tower were gap filled and reformatted so that they could be used as climate forcing
 501 by the ORCHIDEE. Boundary conditions for ORCHIDEE, such as soil texture, pH and soil color were retrieved
 502 from the USDA map, for the corresponding gridcell. The observed land cover and land use for the gridcell were

Table 2: Climate characteristics of the eight locations used in the simulation experiments. The acronyms refer to the site names used in the FLUXNET database (Pastorello et al. 2020).

Site	FI-HYY	DK-SOR	DE-THA	CZ-WET	FR-HES	FR-FON	IT-REN	IT-COL
Full name	Hyytiala	Soroe	Tharandt	Třeboň	Hesse	Fontainebleau	Renon	Collelongo
Country	Finland	Denmark	Germany	Czech	France	France	Italy	Italy
Latitude (°N)	61.84	55.49	50.96	49.02	48.4	48.48	46.59	41.85
Longitude (°E)	24.29	11.64	13.57	14.77	7.1	2.78	11.43	13.59
MAT (°C)	3.8	8.2	8.2	7.7	9.5	10.2	4.7	6.3
MinAT (°C)	-10.8	2.7	-3.9	-5.2	0.1	-1.1	-6.3	-3.8
MAP (mm.y ⁻¹)	522	811	734	587	653	989	752	1050
Mean annual net radiation (w.m ⁻²)	42.1	49.4	52.5	68.0	53.7	50.3	67.7	68.3

503 ignored and set to pure spruce because this study did not investigate the effect of species mixture in the simulation
504 experiments. The resolution of the gridcell chosen for this analysis is 2500 km². Although this corresponds to a high
505 resolution for large-scale simulations with ORCHIDEE it is a coarse resolution for studying bark beetle outbreaks.

506

507 The climate forcings were looped over as much as needed to bring the carbon, nitrogen, and water pools to
508 equilibrium during a 340 years long spinup. Following the spinup, a 100-years simulation was run starting with a
509 windthrow event on the first day of the first year. The results presented in this study come from the 100-years long
510 simulations. Given the focus on even-aged monospecific spruce forests in regions where spruce growth is not
511 constrained by precipitation, variables such as $i_{hosts\ share}$ and $i_{hosts\ defense}$ were omitted from this study. Note that
512 ORCHIDEE does not account for possible acclimation e.g., temporal changes in bark beetle behavior or bark beetle
513 resistance to external stressor such as winter temperature.

514

515 3.2. Selection of locations

516 Bark beetle populations are known to be sensitive to temperature as they are more likely to survive a mild winter
517 (Lombardero et al., 2000) and tend to breed earlier when winter and spring are warmer than usual, allowing for
518 multiple generations in the same year (Hlásny et al., 2021a, also see eq. 10 from section 2.6). In order to assess the
519 temperature effect of the bark beetle outbreak model in ORCHIDEE, eight locations in Europe were selected (Table
520 2) which represent the range of climatic conditions within the distribution area of Norway spruce (*Picea Abies* Karst
521 L.), the main host plant for *Ips typographus*, the bark beetle species under investigation.

522

523 For these eight locations, half-hourly weather data from the FLUXNET database (Pastorello et al., 2020) were used
524 to drive ORCHIDEE. Some of these locations (FON, SOR, HES, COL, WET) are in reality not covered by spruce
525 but all sites are, however, located within the distribution of Norway spruce. In this study, locations were selected to
526 use the observed weather data to simulate a credible temperature and rainfall gradient for spruce. HES location is no
527 longer part of the FLUXNET network but the previous data are still available are relevant for this analysis.

528

529 3.3. Sensitivity to model parameters

530 The sensitivity assessment evaluates the responsiveness of four key variables ($i_{hosts\ susceptibility}$, $i_{beetles\ mass\ attack}$, $i_{beetles}$
531 $generation$, $i_{beetles\ activity}$) of the *Ips typographus* outbreak model implemented in ORCHIDEE. The assessment aims to
532 demonstrate the ability of ORCHIDEE to simulate diverse dynamics of bark beetle infestations. The selection of i_{hosts}
533 $susceptibility$, $i_{beetles\ activity}$, $i_{beetles\ mass\ attack}$, and $i_{beetles\ generation}$ was based on two criteria: (1) their substantial influence on the
534 dynamics of the *Ips typographus* outbreak noted during model development, and (2) their independence from direct
535 measurable data, rendering them less suitable for evaluation through literature review.

536

537 For each of the four variables, three distinct values were assigned to two parameters labeled “Shape” and “Limit”.
538 The *Shape* parameter determines the shape of the logistic relationship, with three values tested: (a) *Shape*=-1.0,
539 yielding a linear relationship, (b) $-5.0 < Shape < -30.0$, resulting in a logistic curve, and (c) *Shape*=-500.0, turning the
540 logistic relationship into a step function. For the logistic curve, the exact *Shape* value between -30.0 and -5.0 is
541 chosen according to each index under study: (1) $S_{susceptibility} = -5.0$; (2) $S_{activity} = -20.0$; (3) $S_{mass\ attack} = -30.0$; and (4)
542 $S_{generation} = 5.0$. For $S_{mass\ attack}$ and $S_{activity}$, higher values have been chosen because the slope of the logistic curve has a
543 significant impact in order to trigger an outbreak.

544

545 The second parameter called “Limit” determines the threshold, derived from expert insights, at which the logistic
546 relationship will reach its midpoint value of 0.5 ($i_{rd\ susceptibility}$, BP_{limit} , Act_{limit} , or G_{limit}). For instance, $i_{rd\ susceptibility}$ is set at
547 0.55, indicating $i_{hosts\ susceptibility}$ midpoint sensitivity (Eq. 6'). Setting BP_{limit} at 0.12 results in an $i_{beetles\ mass\ attack}$ midpoint
548 when $i_{beetles\ pressure}$ is 0.12, selected for its proximity to scenarios where $i_{hosts\ dead}$ equals 1.0 (Eq. 14). Act_{limit} was
549 positioned at 0.06, signifying the $i_{beetles\ activity}$ midpoint at a $DR_{beetles} = 6\%$ from the preceding year, exceeding endemic
550 levels yet not reaching epidemic outbreaks (Eq. 10). Lastly, G_{limit} is fixed at 1.0, denoting the midpoint for $i_{beetles}$
551 $generation$ upon completing one generation annually, underpinning the rarity of bark beetle outbreaks with fewer than
552 one generation per year (Eq. 9). Starting from these reference values, a “restrictive” simulation was run in which the
553 “Limit” parameter values were reduced by 50%. Likewise a “permissive” simulation was run to test 50% higher
554 values for “Limit”.

555

556 The sensitivity analysis of the model parameters explores 36 (3 shapes x 3 limits x 4 equations) combinations of
557 parameters values named “set”, but the full design of the experiment is $8^3=512$ sets (8 parameters, 3 values for each).
558 This deliberate choice has been made because of the computation time cost of a single run. In order to reduce the
559 number of runs from 512 to 36, we had to make simplifications: (1) one equation at the time is studied, reducing to 9

560 the number of sets necessary to realize the sensitivity analysis (2) every other parameters from the remaining
561 equation is set to default value e.g. “Limits” are set to their reference values and “shape” are set to their a priori
562 assumption (table 4). The major drawback of this approach is that interaction effects between equations can not be
563 investigated in the study. Nonetheless, this sensitivity analysis aims to document model behavior, rather than seeking
564 precise parameter values which can be achieved with the main effect of each equation only (see section 3.4).
565 The simulations were run for the THA site, where they were repeated for two prescribed windthrow events with a
566 different intensity, i.e., a $DR_{windthrow}$ of 0.1 and 10%. The effect of the parameters with a negligible windthrow event,
567 i.e., killing only 0.1% of the trees, was tested to confirm that the selected parameters did make ORCHIDEE simulate
568 a bark beetle outbreak in the absence of windthrow (*score5* in section 3.4).

569

570 3.4. Parameter tuning and credibility score

571 The results of the sensitivity experiment were used to select key model parameters. Selecting the values for the
572 *Shape* and *Limit* parameters (see section 3.3) used in the calculation of the variables $i_{hosts\ susceptibility}$, $i_{beetles\ mass\ attacks}$, $i_{beetles}$
573 $generation$, and $i_{beetles\ activity}$ has been carried out in order to reproduce the observed dynamics of bark beetle outbreaks.
574 Observed dynamics were compiled through a literature search for peer-reviewed papers that reported quantitative
575 characteristics of bark beetle outbreaks (Table 3). ~~Four~~Five characteristics could be documented and use to calculate
576 score:

- 577 • The delay between the windthrow event and the start of the bark beetle outbreak (*score1*).
- 578 • The length of the bark beetle outbreak is defined by the number of years required for a bark beetle
579 population to go back to its endemic level (*score2*).
- 580 • The cumulative number of trees per unit area, killed by the bark beetles at the end of an outbreak (*score3*).
- 581 • The average tree mortality rate ($DR_{beetles}$) during an endemic stage (*score4*).
- 582 • No outbreak is triggered when $DR_{windthrow} = 0.1\%$. This characteristic is mandatory in order to avoid
583 outbreak for no specific event (*score5*).

584

585 Based on Table S1 and the reference range in Table 3, scores are calculated for each parameter set and values are
586 either 0 or 1. The Credibility Score (CS) is the sum of four scores, ~~indicating that the result falls within the four~~
587 ~~reference ranges described above and no outbreak is triggered when $DR_{windthrow} = 0.1\%$. The~~ times a fifth
588 score. The CS is computed as follows: $CS = (score1 + score2 + score3 + score4) \times score5$. Only parameter sets
589 achieving a CS of 4 will be selected. If multiple parameter values are possible for a given equation, the most
590 frequently selected value will be preferred.

591

Table 3 : Literature-based summary of characteristics of large-scale bark beetle outbreaks. Due to data scarcity, the characteristics combine outbreak dynamics of different bark beetle species, different host species, and different locations. The reference range is used to calculate the credibility score (CS) of each set of parameters (but see table s1).

Outbreak characteristics	Literature findings	Reference range	How to estimate in ORCHIDEE ?
Delay before the start of an outbreak (build-up)	A notable surge in the population of <i>I. typographus</i> was observed in windthrow areas during the second to third summer following the storm (Havašová et al., 2017; Kärverno and Schroeder, 2010; Wermelinger, 2004; Wichmann and Ravn, 2001).	[2, 3] years, use in the calculation of <i>score1</i>	Using the tree mortality rate by bark beetles ($DR_{beetles}$), one can assess the number of years since the storm before reaching the maximum mortality rate (epidemic stage).
Length of an outbreak (epidemic)	Studies suggest that <i>I. typographus</i> outbreaks in Europe can last anywhere from 11 to 17 years (Bakke, 1989; Hlásny et al., 2021b; Mezei et al., 2014).	[11, 17] years, use in the calculation of <i>score2</i>	Using the tree mortality rate by bark beetles ($DR_{beetles}$), one can assess the number of years past since the storm before reaching the minimum mortality rate (endemic stage).
Severity rate of an outbreak (severity)	A severe bark- <i>D. Ponderosa</i> outbreak resulted in a 52%-60% reduction in tree numbers at large landscape scale (>2000km ²) (Morehouse et al., 2008; Pfeifer et al., 2011) In Wallonia and East France, <i>I. Typographus</i> outbreak resulted in 12.6% reduction of spruce forest area in 6 years (Arthur, G., et al. 2024).	Highly dependent from the size of the forest studied but for a grid cell of 2500km ² , ones could expect a [25%, 45%] reduction over the entire course of a massive outbreak. Use in the calculation of <i>score3</i>	Count the number of trees killed by bark beetles until the end of the outbreak, then divide by the number of trees just after the storm event.
Endemic mortality rate (endemic)	Total background mortality is around 1.2%.year ⁻¹ . Bark beetles as a functional group are estimated to account for 40% of the total mortality in the United States (≈0.5%.year ⁻¹) (Berner et al., 2017; Das et al., 2016; Hlásny et al.,	Not enough data was available to estimate a range. Nonetheless we decided to calculate a range including a 10% uncertainty [0.45-0.55] %.year ⁻¹ . Use in the	After the end of the outbreak, count the number of trees that die every year. Then average it.

592

593 **3.5. Sensitivity to climate and windthrow**

594 In this simulation experiment, the influx of fresh dead tree hosts (N_{wood}) used for bark beetle breeding was controlled
 595 by modifying the maximum damage rate of a windthrow event ($DR_{windthrow}$) in ORCHIDEE. Seven $DR_{windthrow}$ were
 596 simulated (i.e. 0.1%, 5%, 7.5%, 10%, 15%, 20%, 35%). Given the monotonic nature of the relationships between
 597 $DR_{windthrow}$ and $i_{hosts\ dead}$ (Eq. 12), each event triggers a proportional increase in the dead host availability ($i_{hosts\ dead}$)
 598 scaling between 0 and 1 (Fig. 3). Through its equations, ORCHIDEE assumes that for damage rates above 20% the
 599 variable $i_{hosts\ dead}$ (N_{wood}) will always be equal to 1.0. $i_{rd\ spruce}$ however, may further decrease with increasing
 600 windthrow damage, which makes the 35% damage rate still interesting to investigate. Although the simulations were
 601 run for all $DR_{windthrow}$, only four windthrow damage rates including a windstorm resulting in a 35% damage rate (Fig.
 602 3), were presented to enhance the readability of the result section.

603

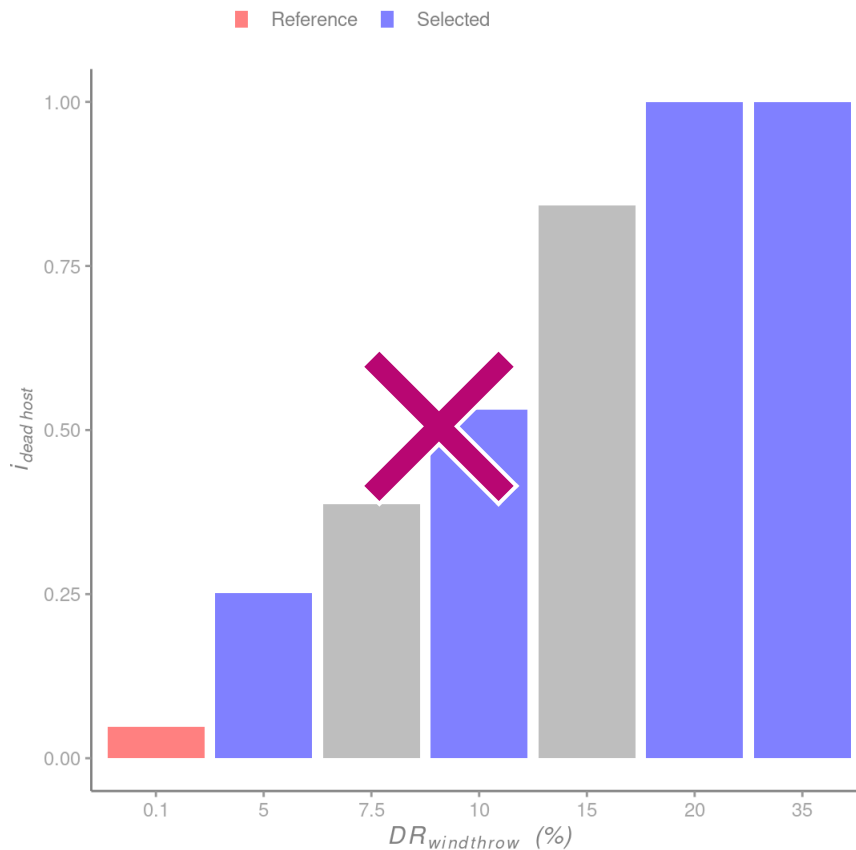


Figure 3: Relationship between windthrow damage rate ($DR_{windthrow}$) and dead host index ($i_{hosts\ dead}$). For each site a $DR_{windthrow} = 0.1\%$ was used as the reference simulation

because an endemic bark beetle population is expected following such a low intensity windthrow event. The four $DR_{windthrow}$ shown in blue were selected for subsequent presentation of the results because they cover the entire range for the $i_{hosts\ dead}$.

604

605 The main driver of the number of generations a bark beetle population can achieve in one year is the number of days
606 higher than 8.3°C during winter time (Temperli et al., 2013) which is the reason why temperature is so important for
607 bark beetle reproduction. By taking REN, THA, WET and HES, the number of bark beetle generations ranged from
608 0.8 to 3.5 (Fig. 4) which is similar to the number of generations observed across Europe (Faccoli and Stergulc, 2006;
609 Jönsson et al., 2009, 2011). Limiting the analysis to only four sites simplifies the presentation without affecting the
610 range under investigation.

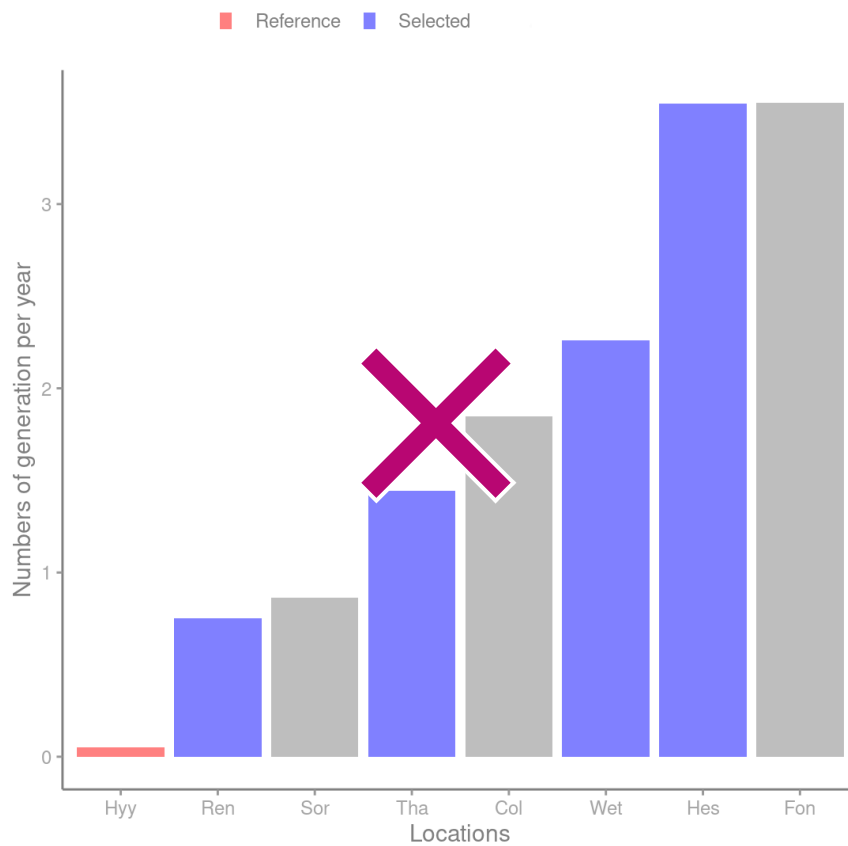


Figure 4: Average number of bark beetle generations during the 5 years following the wind storm for at eight locations along a climate gradient. The HYY location in Finland was selected as the reference for the REN, THA, WET and HES locations. Only results from the reference and four selected locations (shown in blue) are shown in the results to enhance readability.

611

612 For the climate gradient, the simulation for HYY served as a reference since the number of generations is lower than
613 1 for which no outbreak should happen under any circumstances. Under present climate conditions, an outbreak in
614 HYY should be considered an undesirable model result. Likewise, a $DR_{windthrow}=0.1\%$ is considered too low to trigger
615 an outbreak and was therefore used as the reference for the wind damage rate tests.

616

617 The experiment consisted of 40 simulations, i.e., 8 sites (including the reference) x 5 wind damage rates (including
618 the reference). Although the simulations were also run for SOR, COL and FON their results were found to be too
619 similar to the results of selected sites to present them as well. Hence, the result section presents only 25 out of the 40
620 simulations. Three output variables were assessed: bark beetle damage rate ($DR_{beetles}$), total biomass (B_{total}), and net
621 primary production (NPP). Total biomass was investigated over 100 years whereas $DR_{beetles}$ and NPP were assessed
622 for the first 20 years following a windthrow.

623

624 **3.6. Continuous vs abrupt mortality**

625 Where most land surface models use a fixed turnover time to simulate continuous mortality (Pugh et al., 2017;
626 Thurner et al., 2017), ecological reality is better described by abrupt mortality events. An idealized simulation
627 experiment was used to qualify the impact of abrupt mortality on net biome productivity by changing from a
628 framework in which mortality is approximated by a constant background mortality to a framework in which
629 mortality occurs in abrupt, discrete events. The impact of a change in mortality framework was assessed with an
630 idealized simulation experiment that compares three configurations of ORCHIDEE: (1) a configuration that
631 simulates mortality as a continuous process, labeled "the continuous configuration" which corresponds to previous
632 versions of ORCHIDEE, and (2) a configuration capable of simulating abrupt mortality from windthrow and
633 subsequent bark beetle outbreaks, labeled "the abrupt configuration" and (3) a configuration in which windthrow is
634 activated but bark beetles outbreak is implicitly accounted for in the background mortality. This third configuration
635 enabled attributing the impact to windthrow. The effect of simulating abrupt mortality was evaluated over 20, 50,
636 and 100 year time horizons.

637

638 The impact of changing the mortality framework from continuous to abrupt was quantified on the basis of 120
639 simulations (8 locations x 7 windthrow damage rates x 2 configurations + 8 sites x 1 configuration) of 100 years
640 each.

641

642 The simulations with abrupt mortality were run first. Subsequently, the number of trees killed was quantified and
643 used as a reference value for the continuous mortality set-up. This approach resulted in the same quantities of dead
644 trees at the end of the simulation for both frameworks, which then differed only in the timing of the simulated
645 mortality. This precaution is necessary to avoid comparing two different mortality regimes where the result would
646 mainly be explained by the intensity of the mortality rather than by its underlying mechanisms.

647

648 Changes in forest functioning were evaluated through the temporal evolution of accumulated net biome productivity
649 (*NBP*) over a 100-years time frame. *NBP* is defined as the regional net carbon accumulation after considering losses
650 of carbon from fire, harvest, and other episodic disturbances. In ORCHIDEE, *NBP* is calculated following the
651 definition by Chapin et al. (2006) as the carbon remaining in the biomass, litter and soil after accounting for
652 photosynthesis, and respiration because fire, harvest, leaching and volatile emissions were not accounted for in this
653 simulations experiment.

654

655 4. Results

656 4.1. Sensitivity to model parameter sets

657 The impact of spruce stand competition ($i_{hosts\ susceptibility}$) on outbreak dynamics was examined by adjusting the
658 parameters $S_{susceptibility}$ and $i_{rd\ susceptibility}$ in equation 6a'. When $S_{susceptibility}$ resulted in a linear relationship ($S_{susceptibility} =$
659 -1.0), no peak in bark beetle damage occurred for the three tested values of $i_{rd\ susceptibility}$ (permissive, reference,
660 restrictive) at a 10% windthrow damage rate (Fig. 5, panel h). However, employing a step function ($S_{susceptibility} =$
661 -500.0) led to either sporadic peaks of bark beetle damage with a permissive $i_{rd\ susceptibility}$ or a two-year outbreak with a
662 maximum damage rate of 60% with a restrictive $i_{rd\ susceptibility}$ (Fig. 5, panel h), neither of which aligns with the
663 observations summarized in Table 3.

664

665 The closest outcome to observation from table 3 was obtained with a logistic relationship ($S_{susceptibility} = -5.0$), where
666 $i_{rd\ susceptibility}$ determined the duration of the outbreak: 11, 16, and 25 years for restrictive, reference, and permissive
667 parameter values, respectively (Fig. 5, panel h). Either the restrictive or reference parameter value could be utilized
668 since a range of 11-16 years aligns with the observations (Table 3). To examine the occurrence of improbable
669 outbreaks, sensitivity tests were repeated for a 0.1% windthrow damage rate. None of the nine parameter
670 combinations triggered an outbreak (Fig. 5, panel g), suggesting that improbable outbreaks due to the calculation of
671 $i_{hosts\ susceptibility}$ are unlikely.

672

673 From the calculation of the credibility score, only one set obtains a score of 4 ($S_{susceptibility} = -5.0$, $i_{rd\ susceptibility}=0.55$,
674 Table s1). The concerning parameters value has been selected and reported in table 4.

675

676 The effect of the capability of bark beetle to mass attack ($i_{beetles\ mass\ attack}$) when the population exceeds a threshold was
677 evaluated by varying $S_{mass\ attack}$ and BP_{limit} (Eq. 14). Linear relationships ($S_{mass\ attack} = -1.0$) resulted in similar outbreak
678 dynamics for all BP_{limit} values, with the model settling on a constant endemic damage following an outbreak, though
679 higher than observed (Table 3, Fig. 5, panel f). Introducing a logistic or step function slightly altered outbreak
680 dynamics except when assuming a step function for the restrictive value, which prevented an outbreak. Repeating
681 sensitivity tests for a 0.1% windthrow damage rate showed that assuming linear or logistic relationships could trigger
682 an outbreak (Fig. 5, panel e), indicating that improbable outbreaks may arise from the calculation of $i_{hosts\ mass\ attack}$.

683

684 From the calculation of the credibility score, three sets obtain a score of 4 but only set 4.6 was chosen because of its
685 intermediate position compared to sets 4.9 and 4.5 (Table s1). The concerning parameter values ($S_{mass\ attack} = -30.0$,
686 $BP_{limit} = 0.06$) have been selected and reported in table 4.

687

688 The impact of bark beetle activities from the previous year ($i_{beetles\ activity}$) on outbreak dynamics was investigated by
689 varying $S_{activity}$ and act_{limit} (Eq. 10). Linear or logistic relationships resulted in excessively long outbreaks (>30 years)
690 compared to observations (Table 3, panel b), whereas assuming a step-function relationship simulated a decline in
691 the outbreak after 14 years. Sensitivity tests repeated for a 0.1% windthrow damage rate showed that assuming a
692 linear relationship could trigger an improbable outbreak (Fig. 5, panel a) through the calculation of $i_{beetles\ activity}$.

693

694 From the calculation of the credibility score, only one set obtains a score of 4 ($S_{activity} = -500.0$, $act_{limit} = 0.12$, Table
695 s1). The concerning parameters value has been selected and reported in table 4.

696

697 To explore the effect of the numbers of generation ($i_{beetles\ generation}$) on the outbreak dynamics, $S_{generation}$ and G_{limit} from
698 equation 9 were varied. Bark beetle damage rate was more sensitive to G_{limit} than $S_{generation}$, but only a linear
699 relationship with the reference $G_{limit} = 1.0$ yielded an intermediate outbreak intensity consistent with the continental
700 climate at the test location (i.e., THA, Fig. 5, panel d). Other combinations resulted in either too strong or no peak
701 during the outbreak. Repeating sensitivity tests for a 0.1% windthrow damage rate showed that none of the nine
702 parameter combinations triggered an outbreak (Fig. 5 panel c), indicating that improbable outbreaks from the
703 calculation of $i_{beetles\ generation}$ are unlikely.

704

705 From the calculation of the credibility score, three sets obtain a score of 4 but only set 1.4 was chosen because of its
706 intermediate position compared to sets 1.1 and 1.5 (Table s1). The concerning parameter values ($S_{generation} = 1.0$,
707 $G_{limit} = 1.0$) have been selected and reported in table 4.

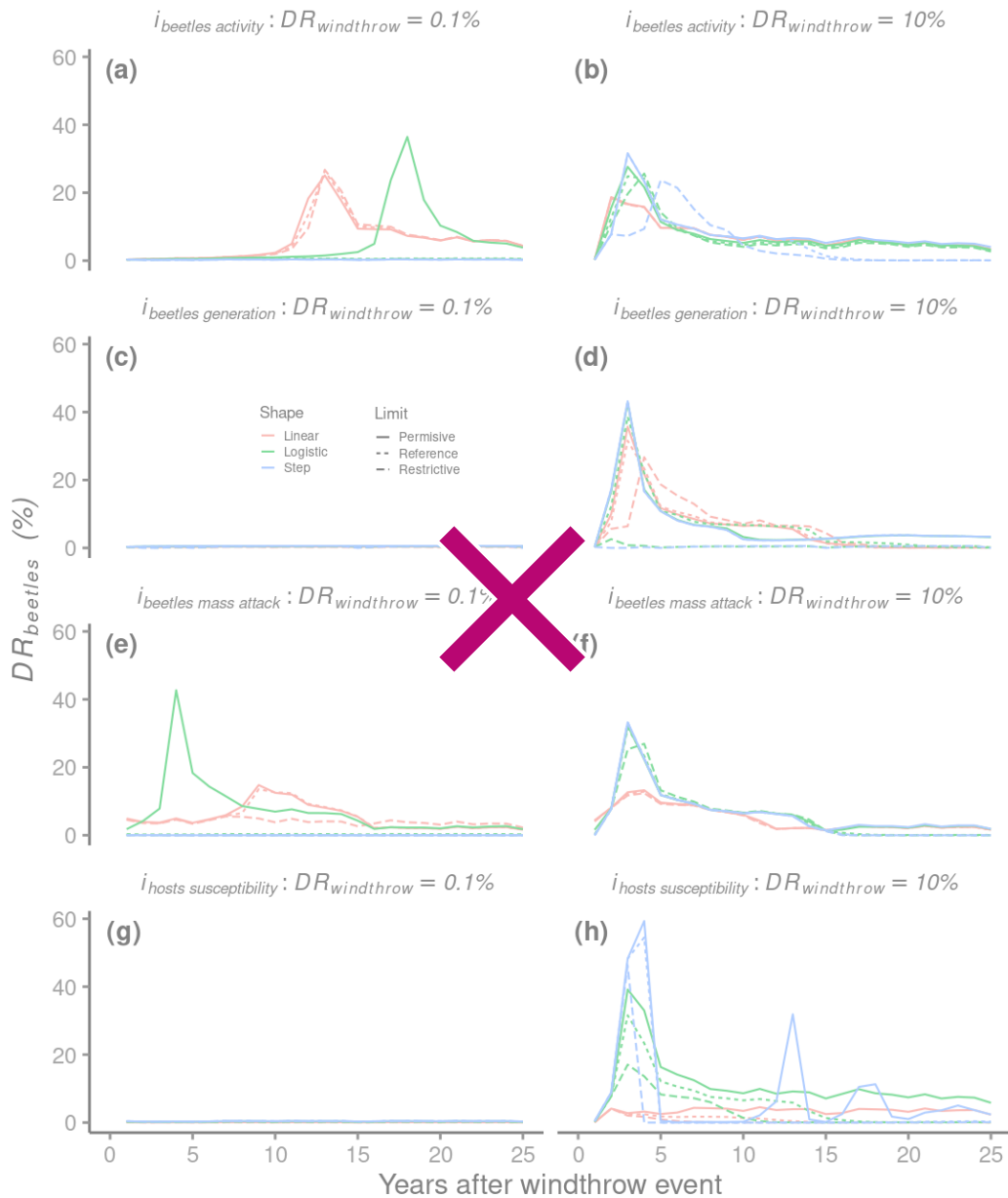


Figure 5: Simulation results from the sensitivity experiment at the THA site. Eight parameters from four equations were evaluated. Each equation represents an index from the bark beetle outbreak model ($i_{hosts\ susceptibility}$, $i_{hosts\ mass\ attack}$, $i_{beetles\ activity}$, $i_{beetles\ generation}$). Each index is represented by a logistic function defined by a shape parameter (*Shape*) and a limit parameter (*Limit*). Three values were chosen for each parameter resulting in 9 pairs of parameters for each index. Colored lines represent the shape parameter varying from linear : $Shape = -1.0$ (red), logistic $-5.0 < Shape < -30.0$ (green), to step function where $Shape = -500.0$ (blue). Line type represents three different values for *Limit* parameters where references (dashed line) are values of $i_{rd\ susceptibility}$, BP_{lim0} , act_{limit} and G_{jimit} (given in table 4), whereas permissive (full line) and restrictive (dashed dotted) represent a 50% decrease or increase respectively.

708

709

4.2. Model tuning

710 By comparing the outcomes of the sensitivity tests (section 4.1) to a compilation of observations (Table 3), a first
 711 estimate for several parameters was proposed (Table 4). Details about the other values used in the sensitivity test can
 712 be found in table S1.

713

Table 4: Parameter values from the bark beetle model based on the score obtained in the sensitivity analysis. (*) parameter values deliberately fixed and excluded from the sensitivity analysis (section 3.3 for justification).

Parameter	Source	Chosen parameters
$S_{generation}$ act_i $limit$	This study: from SA (see 3.1.4 3.1.3)	1.0 0.06
G_{limit} BP_{limit}	Adapted from Temperli et al. 2013 This study: scale dependent (see 3.1.2)	1.0 0.12
DD_{ref}	Adapted from Temperli et al. 2013	547.0 (*)
$S_{drought}$ G_{limit}	Adapted from Temperli et al. 2013	0.5 (*) 1.0
PWS_{limit} i_{rd} $limit$	Adapted from Temperli et al. 2013 This study: scale dependent (see 2.4.1)	0.4 (*)
max_{Nwood} i_{rd} $susceptibility$	This study: scale dependent from SA (see 2.4.23.1.1)	0.2 (*) 0.55
$S_{activity}$ max_N $wood$	This study: from SA scale dependent (see 3.1.32.4.2)	500.0 0.2 (*)
act_{limit} PWS_i $limit$	This study: from SA (see 3.1.3) Adapted from Temperli et al. 2013	0.06 0.4 (*)
$S_{susceptibility}$ S_a $ctivity$	This study: from SA (see 3.1.1 3.1.3)	20.0 500.0
i_{rd} $susceptibility$ S_{dro} $ught$	This study: from SA (see 3.1.1) Adapted from Temperli et al. 2013	0.55 -9.5 (*)
$S_{competition}$ S_{su} $sceptibility$	This study: from SA (see 3.1.1)	5.0 (*) 20.0
i_{rd} $limit$ $S_{competition}$	This study: scale dependent from SA (see 2.4.13.1.1)	0.4 5.0 (*)
$S_{mass\ attack}$	This study: From SA (see 3.1.2)	-30.0
BP_{limit} S_{genera} $tion$	This study: scale dependent from SA (see 3.1.23.1.4)	0.12 1.0
S_{share}	This study: not used (see 2.5)	15.5 (*)
SH_{limit}	This study: not used (see 2.5)	0.6 (*)

714

715

4.3. Impact of climate and windthrow on bark beetle damage

716 In ORCHIDEE, the warmest sites, HES and WET, experienced significant bark beetle outbreaks across a wide
717 spectrum of windthrow mortality rates, whereas colder sites like REN and THA saw outbreaks only in response to
718 the most severe windthrow events (Fig. 6, panel b, c). A greater average number of bark beetle generations in the
719 years following windthrow events led to higher bark beetle damage rates at the peak of outbreaks. For instance, at a
720 35% windthrow mortality rate, HES reached a maximum bark beetle damage rate of 50%, whereas REN's maximum
721 was 22% (Fig. 6 panel a, b).

722

723 Interestingly, high tree mortality rates from windthrow could also lead to delays and lower maximum $DR_{beetles}$ (Fig.
724 6). For instance, at the HES site, 10%, 20%, and 35% windthrow damage rates triggered maximum $DR_{beetles}$ of 50%,
725 43%, and 37%, respectively (Fig. 6 panel a). Conversely, low $DR_{windthrow}$, like 5% at WET, delayed the peak of bark
726 beetle outbreaks by 9 years (Fig. 6, panel d). Additionally, the model simulated a post-epidemic stage during which
727 the outbreak damage rate remained relatively low (<10%) and lasted between 3 to 10 years (Fig. 6). Overall, the
728 simulated outbreaks lasted between 11 to 20 years, consistent with field observations (Table 3).

729

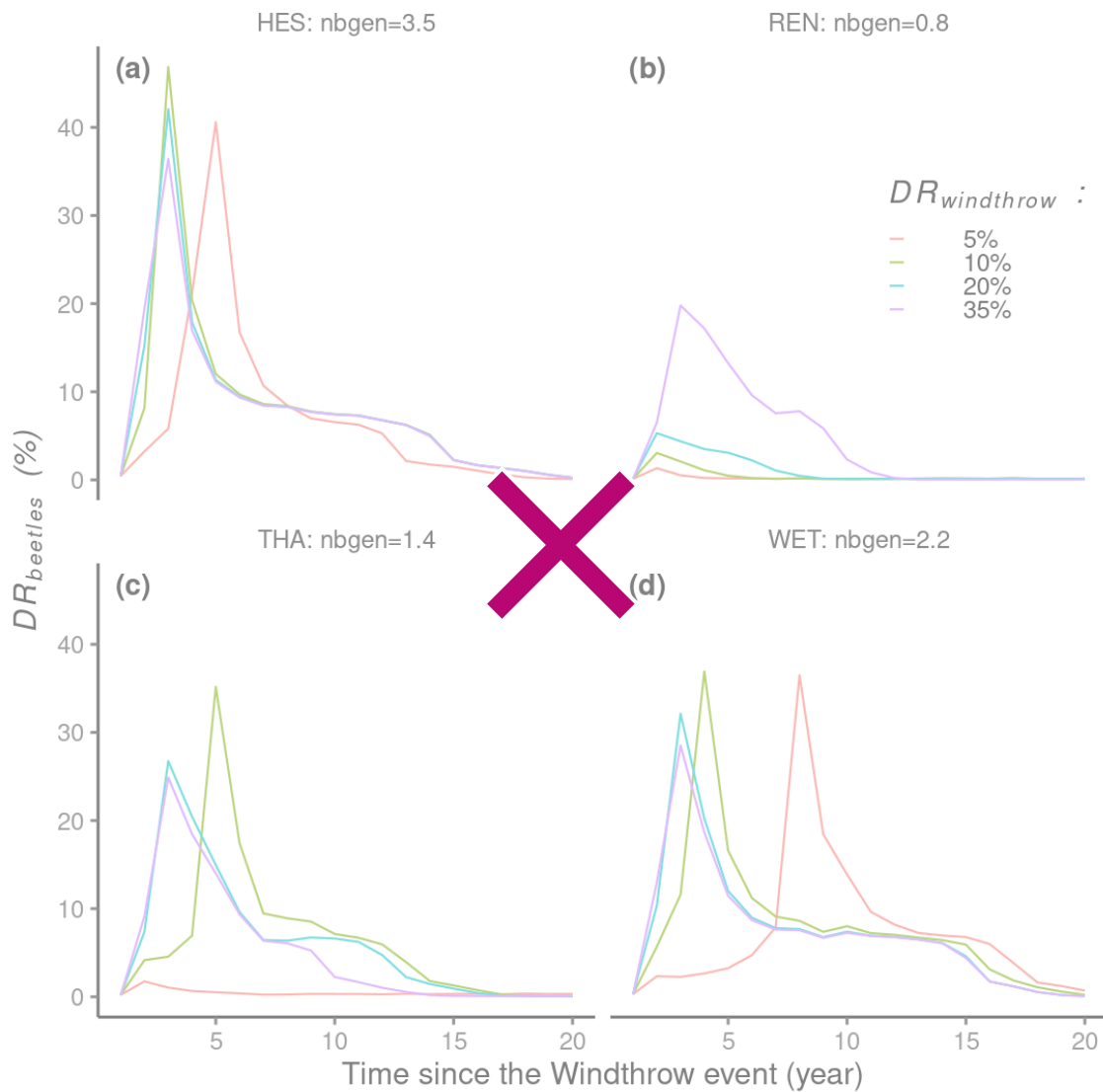


Figure 6: Simulation results of 16 simulations (4 locations x 4 windthrow damage rates $DR_{windthrow}$). Lines represent the annual bark beetle damage rate as a fraction of the total biomass ($DR_{beetles}$). $Nbgen$ is the average number of bark beetle generations during five years after the windthrow event. $DR_{windthrow}$ represents the percentage of biomass loss by a windthrow event at the start of the simulation.

730

731 At the coldest site, HYY, ORCHIDEE simulated only a small number of bark beetle generations, preventing
 732 outbreaks from occurring. This observation validates the initial parameter tuning (Table 4), indicating that it is robust
 733 enough to prevent improbable outbreaks, such as the model triggering outbreaks in sites where bark beetles cannot
 734 reproduce.

735

736

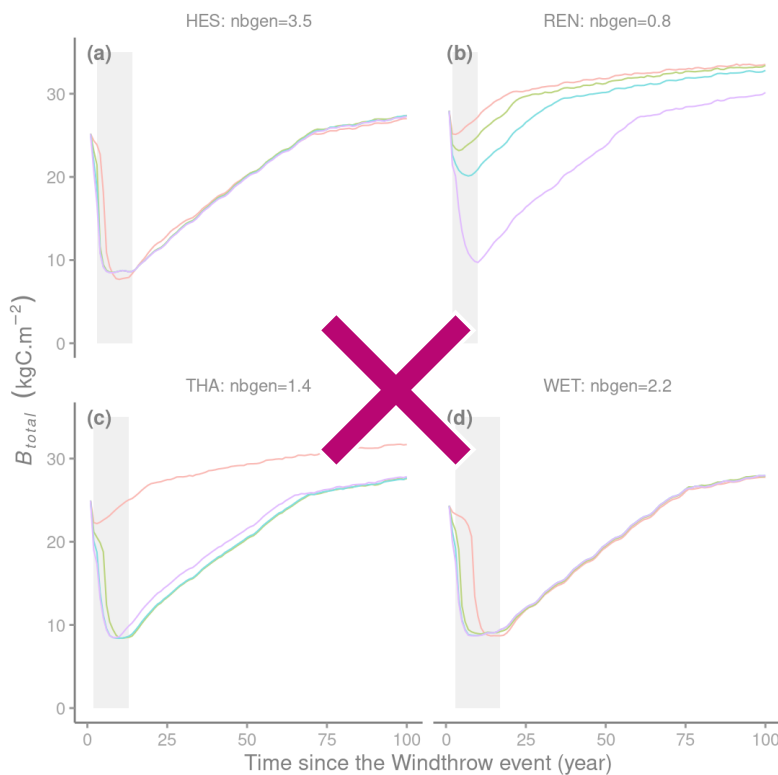
4.4. Impact of climate and windthrow on stand biomass and Net Primary Production

737 All locations experienced a 10 to 20 years decrease in total biomass until at most 9 kgC.m⁻² at which time the
 738 outbreak ended (Fig. 7, panel a, b, c, d). The model can simulate significant epidemic events even if the initial
 739 trigger, such as the windthrow event in our study, is not particularly intense. Once the bark beetles can mass attack
 740 living trees, the bark beetle population ($i_{beetles\ pressure}$) will increase and kill more and more trees until so many trees are
 741 killed that the stand density of the remaining living trees drops below the threshold of $i_{rd\ spruce} = i_{rd\ limit}=0.4$. In
 742 ORCHIDEE, an $i_{rd\ limit}=0.4$ for spruce forest corresponds to a biomass of around 9 kgC.m⁻² which in ORCHIDEE is
 743 too low to maintain an epidemic population of bark beetles at the 2500 km² grid cell. Interestingly, for the climate
 744 observed at REN where the number of generations is approximately one, the bark beetle population can only
 745 become epidemic following an intense windthrow event with a 35% damage rate (Fig. 7).

746

747 Throughout the outbreak period, there was a notable decrease in net primary production (*NPP*)(Fig. 7). This decrease
 748 is primarily attributed to a sharp decline in leaf area index (not shown). Following the epidemic phase, the leaf area
 749 recovers. Following the outbreak: the reduction in stand tree density due to bark beetle damage decreases autotrophic
 750 respiration (not shown) and the sparser canopy allows more light to reach the forest floor where it fosters
 751 recruitment (not shown), resulting a higher *NPP* or forest growth (Fig. 7). Consequently, carbon use efficiency tends
 752 to be higher in sparsely populated stands compared to densely populated ones.

753



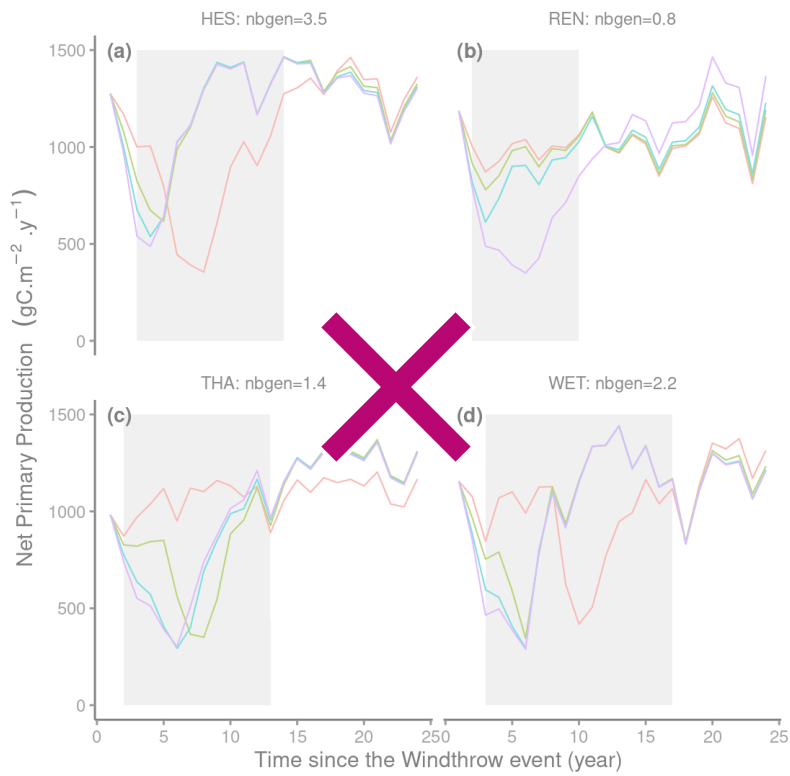


Figure 7: Simulation results of 16 simulations (4 sites x 4 windthrow mortality rate). Lines represent the annual average net primary production (NPP) in $\text{gC}\cdot\text{m}^{-2}\cdot\text{y}^{-1}$ or total stand biomass (B_{total}) in $\text{kgC}\cdot\text{m}^{-2}$. $Nbgen$ is the average number of bark beetle generations during the five years after the windthrow event. $DR_{windthrow}$ represents the percentage of biomass loss by a windthrow event at the start of the simulation. Grey areas represent the epidemic phase.

754

755

4.5. Continuous vs. abrupt mortality

756

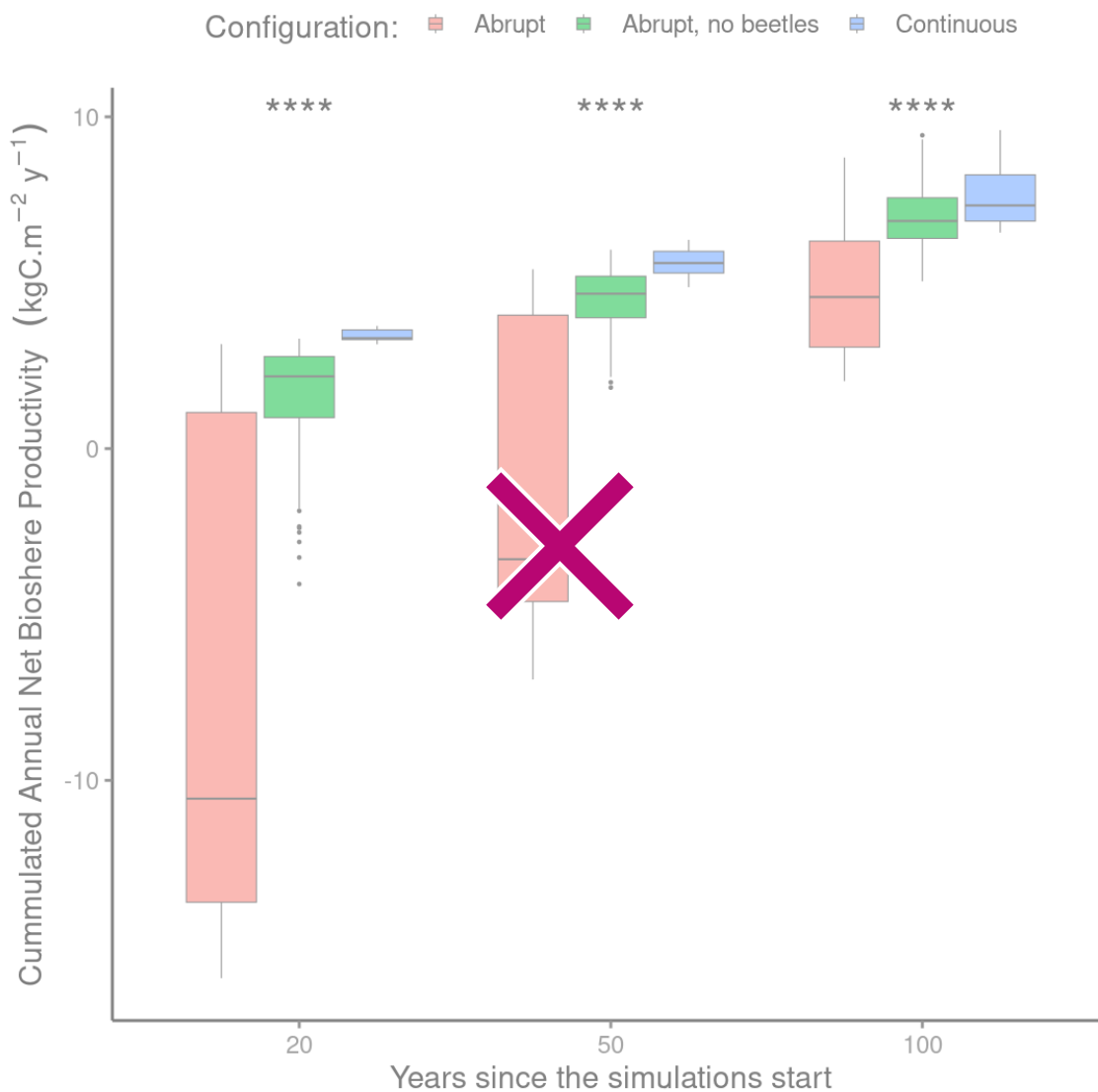


Figure 8: Difference in cumulative net biome production at three discrete time horizons (i.e. 20, 50 and 100 years) between a fixed continuous mortality rate (blue, n=8), abrupt tree mortality from a windstorm and the subsequent bark beetle outbreak (red, n=56), abrupt mortality from a windstorm not followed by a bark beetles outbreak (green, n=56). Note that in the continuous mortality configuration the mortality rate was adjusted to obtain a similar number of trees killed after 100 years as in the abrupt mortality configuration. The variation of each boxplot arises due to different locations and prescribed storm intensities. Each boxplot displays the median value (thick horizontal line), the quartile range (box border), and the 95% confidence interval (vertical line). A Wilcoxon test between the three configurations at each time horizon showed significant differences (p-value<0001) denoted by the four stars.

757 The total accumulated net biome production (*NBP*) was evaluated using the ORCHIDEE model across three
 758 different timeframes: 20, 50, and 100 years. At the 20-years mark, the average accumulated *NBP* notably differed

759 between the 'continuous', 'abrupt' and the abrupt without bark beetles outbreak ('no beetles') mortality
760 configurations: -7.12 ± 0.97 , -1.37 ± 0.28 and 3.39 ± 0.74 $\text{kgC.m}^{-2}.\text{y}^{-1}$ for the 'abrupt', 'no beetles' and 'continuous'
761 mortality configurations, respectively. These differences were statistically significant (Wilcoxon, p -value <0.001),
762 indicating a substantial initial reduction in *NBP* with the 'abrupt' configurations, as ecosystems behaved as carbon
763 sources, whereas under the 'continuous' configuration, they acted as carbon sinks (Fig. 8). The variability in *NBP*
764 demonstrated the broad temperature gradient in Europe and indicated that despite many locations potentially acting
765 as sources under the 'abrupt' configuration, some may transition to carbon sinks within the first 20 years following a
766 disturbance.

767

768 Moving to the 50-years horizon, the difference between the three frameworks decreased, with net biome productions
769 of -0.81 ± 0.60 , 4.43 ± 0.15 and 5.61 ± 0.18 $\text{kgC.m}^{-2}.\text{y}^{-1}$ for the 'abrupt', 'no beetles' and 'continuous' mortality
770 configuration, respectively. The difference in sink strength remained statistically significant (Wilcoxon,
771 p -value <0.001), with the *NBP* in the 'abrupt' configuration approaching carbon neutrality while without the
772 consecutive bark beetles outbreak the ecosystems already became a carbon sink. The climate conditions had a lasting
773 effect on the responses, with the 'abrupt' configuration showing a greater range in responses compared to the
774 'continuous' one.

775

776 At the 100-years mark, the average cumulative *NBP* for the 'abrupts' and 'continuous' configurations approached
777 each other with values of 4.85 ± 0.26 , 7.09 ± 0.17 and 7.73 ± 0.40 $\text{kgC.m}^{-2}.\text{y}^{-1}$, respectively (Fig. 8) but were still
778 significantly different (Wilcoxon, p -value <0.001). ORCHIDEE simulated a return to a carbon sink (indicated by
779 positive cumulative *NBP* values) suggesting a long-term recovery and potential return to pre-disturbance
780 productivity levels within a century following the windthrow and beetle outbreak event. The 'continuous'
781 configuration displayed a consistently higher median value, suggesting weaker impact of tree mortality dynamics on
782 the long term carbon cycle.

783

784 5. Discussion

785 5.1. Simulating the dynamics of bark beetle outbreaks and their interaction with windthrow

786 Our *Ips typographus* outbreak model has demonstrated its capability to simulate a broad range of disturbance
787 dynamics. The variation in the outbreak dynamics and the response of the outbreak to its main drivers (Fig. 5 & 6)
788 give confidence in the ability of ORCHIDEE to simulate various outbreak scenarios observed across the temperate
789 and boreal zones under changing climate conditions.

790

791 Windthrow events have significant ecological impact because such disturbances offer fresh breeding substrates,
792 which in turn increase bark beetle populations (Lausch et al., 2011). Our model results align with these findings,
793 indicating that windthrows causing damage of 5% or more may trigger beetle outbreaks (Fig. 6). Additionally, a
794 strong increase in bark beetle populations has been observed following a windthrow event (Wermelinger, 2004), a
795 pattern reflected in the ORCHIDEE simulations. The model simulates a buildup stage spanning 1 to 9 years, where

796 bark beetle numbers increase prior to peaking, with the duration influenced by the severity of the windthrow and the
797 prevailing climate (Fig. 6).

798

799 Temperature is another critical factor affecting bark beetle life cycles. Intra- and interannual variation in temperature
800 impact bark beetles, with warmer conditions fostering multiple generations per year, whereas cooler, damp climates
801 slow breeding and survival rates (Benz et al., 2005). In line with these findings, the temperature dependence of the
802 ORCHIDEE simulations show that cold winters at locations such as SOR and REN reduced bark beetle activity
803 compared to warmer locations like THA and WET (Fig. 6). Lieutier et al. (2004) documented that if the population
804 is large enough, bark beetles can mass attack healthy trees. Our model incorporates this dynamic, illustrated by
805 epidemic stages where living trees become viable hosts, which then exacerbates the growth of the beetle population
806 (Fig. 1).

807

808 The aftermath of a windthrow and subsequent bark beetle outbreak also affects the forest carbon and nitrogen cycles.
809 This impact is observed in the form of snags which are standing dead trees that undergo decomposition. Snags can
810 temporarily disrupt the link between soil and ecosystem carbon and nitrogen dynamics (Rhoades, 2019; Custer et al.,
811 2020). While in ORCHIDEE, the decay of fallen logs does not account for snags yet, the model suggests a recovery
812 period ranging from 5 to 15 years, contingent upon the intensity of the bark beetle outbreak (Fig. 7). As snags create
813 gaps in the canopy, conditions favorable to natural forest regeneration emerge (Jonášová and Prach, 2004) .

814

815 **5.2. Emerging properties from interacting disturbances**

816 While this study did not precisely quantified the impact of simulating abrupt mortality rather than approaching
817 mortality as a continuous process, it demonstrated that the impact of abrupt mortality varies across location and time,
818 i.e. ecosystem functions, such as carbon storage, are affected by natural disturbances like *Ips typographus* outbreaks,
819 having significant impacts on short to mid-term carbon balance estimates (Fig. 8). The simulation experiments also
820 highlighted that the legacy effects of disturbances can endure for decades; even for a simplified representation of
821 forest ecosystems such as ORCHIDEE, where the recovery might be too fast due to the absence of snags (Senf et al.,
822 2017).

823

824 The ability to simulate resistance (i.e., staying essentially unchanged despite the presence of disturbances; Grimm
825 and Wissel, 1997) as an emerging property is evident from Figs. 6 and 7 for ~~locations~~ REN, where no bark beetle
826 outbreaks were observed following a medium windthrow event (5%-20%). However, in all simulated locations that
827 could not resist a bark beetle outbreak, the forest was resilient (i.e., returning to the reference state or dynamic after a
828 temporary disturbance; Grimm and Wissel, 1997) and ecosystem functions were restored to the level from before the
829 windthrow. The elasticity (the speed of return to the reference state or dynamic after a temporary disturbance;
830 Grimm and Wissel, 1997) of the carbon sink capacity ranged from 7 to 14 years. This elasticity is in line with the
831 little observational evidence of ecosystem shifts due to natural disturbances in forests (Millar and Stephenson, 2015).

832 Finally, after the disturbance and the recovery of vegetation structure, the ecosystems simulated by ORCHIDEE
833 showed persistence (i.e. continue along their initial developmental path; Grimm and Wissel, 1997).

834

835 **5.3. Are cascading disturbances important for carbon balance estimates ?**

836 The enhanced complexity introduced into the ORCHIDEE model by incorporating abrupt mortality events, as
837 opposed to a continuous mortality, prompts the question: does this model refinement yield new insights into carbon
838 balance estimates? Our century-long analysis demonstrated that the net biome production, a the metric for carbon
839 sequestration, ultimately converges between the continuous and abrupt mortality frameworks (Fig. 8). This suggests
840 that irrespective of the nature of the mortality events, the forest ecosystem goes through a recovery phase, marked by
841 increased growth that compensates for the growth deficits during the disturbance.

842

843 Yet, our experiment has not taken into account the frequency of disturbances. Given the profound influence of
844 disturbance legacies on carbon dynamics, a recurrence interval shorter than the recovery time of the forest might
845 result in a tipping point. Such a scenario could diminish the carbon sequestration potential of the forest beyond
846 100-year timeframe, and in extreme cases, may even lead to ecosystem collapse, outcomes not explored in the
847 current simulations nor documented in the recent literature (Millar and Stephenson, 2015).

848

849 In the mid-term, spanning 20 to 50 years, the widely used continuous mortality model appears to inflate the carbon
850 sink capabilities of forests when juxtaposed with abrupt mortality scenarios. Since policy frameworks, including the
851 Green Deal for Europe (2023) and the Paris Agreement [(UNFCCC, 2023), upon these medium-term predictions,
852 they would benefit from adopting model simulations that integrate abrupt mortality events to avoid an
853 overestimation of carbon sink capacities of forest. Furthermore, the accuracy of carbon balance estimates strongly
854 depends upon the initial state of the forest in the model. Forest conditions markedly affect carbon uptake rates. Thus,
855 incorporating an abrupt mortality framework into the ORCHIDEE model could substantially refine and strengthen
856 the predictive power of our carbon balance assessments across short, medium, and long-term scales.

857

858 However, it is important to note that the global-scale NBP might not be significantly impacted by abrupt
859 disturbances compared to continuous ones. This is because the scale is so vast that abrupt mortality events are
860 constantly occurring somewhere on the planet, which smooths out the effects illustrated in Figure 8.

861

862 **5.4. Shortcomings of the bark beetle outbreak model**

863 The bark beetle outbreak model developed in this study builds upon the strengths of the previously established
864 LandClim model, though it also inherited some of its limitations. One notable shortcoming is the model for bark
865 beetle phenology, which is an empirical model making use of accumulated degrees-days. Since the conception of the
866 phenology model a decade ago, Europe's climate has undergone substantial changes, primarily manifested in warmer
867 winters and springs (Copernicus, 2024). Because of these changes, chances have increased for two or even more

868 bark beetle generations within a calendar year (Hlásny et al., 2021a). These changes call for an update of the beetle's
869 phenology model to align with these more recent observations (Ogris et al., 2019).

870

871 A second limitation is that our study, ORCHIDEE, has been parameterized to simulate only *Ips typographus* in
872 Europe. In order to change the beetles and tree host interactions e.g. pine bark beetle in North America
873 (*Dendroctonus monticolae* Hopkins), the sensitivity of indexes must be revised, for example, pine beetle is not
874 breeding on the dead wood falling from withrow but very sensitive to drought events (Preisler et al., 2012). $i_{hosts\ defense}$
875 and $i_{hosts\ dead}$ as well as the phenology model will need to be revised.

876

877 Another issue is the model's consideration of drought. As outlined in the method section, drought is treated as an
878 exacerbating factor, rather than a primary trigger as is the case for windthrow. This understanding was accurate for
879 *Ips typographus* a decade ago (Temperli et al., 2013); however, emerging evidence increasingly suggests that
880 drought events may indeed trigger bark beetle outbreaks across Europe (Nardi et al., 2023; Netherer et al., 2015).
881 Consequently, this extreme drought as a trigger should be incorporated in a future revision of ORCHIDEE's *Ips*
882 *typographus* outbreak model.

883

884 6. Outlook

885 This study simulated the one-way interaction between windthrow and *Ips typographus* outbreaks in unmanaged
886 forests. Future research will incorporate additional interactions, such as: the interplay between droughts, storms, and
887 bark beetles; storms, bark beetles, and fires; as well as forest management, storms, and bark beetles.

888

889 The bark beetle outbreak model could also be enhanced by simulating: (a) standing dead trees (or snags), which
890 would help account for differences in wood decomposition between snags and logs (Angers et al., 2012; Storaunet et
891 al., 2005), (b) the migration of bark beetles to neighboring locations, which becomes significant to account for in a
892 model that operates at spatial resolutions below approximately 10 kilometers, and (c) an up-to-date beetle phenology
893 model which accounts for the recent change in their behavior induced by climate change.

894

895 This research provided an initial qualitative assessment of a new model feature. However, the application of the
896 model necessitates an evaluation of the simulations against observations of cascading disturbances at the regional
897 scale, which is the topic of an ongoing study.

898

899 7. Conclusion

900 Our approach enables improving the realism of the *Ips typographus* model in ORCHIDEE without reducing its
901 generality (Levins, 1966). The integration of a bark beetle outbreak model in interaction with other natural
902 disturbance such as windthrow into the ORCHIDEE land surface model has resulted in a broader range of
903 disturbance dynamics and has demonstrated the importance to simulate various disturbance interaction scenarios
904 under different climatic conditions. Incorporating abrupt mortality events instead of a fixed continuous mortality

905 calculation provided new insights into carbon balance estimates. The study showed that the continuous mortality
906 framework, which is commonly used in the land-surface modeling community, tends to overestimate the carbon sink
907 capacity of forests in the 20 to 50 year range in ~~ecosystems under high~~ region/area under the same disturbance
908 pressure, compared to scenarios with abrupt mortality events.

909

910 Apart from these advances, the study revealed possible shortcomings in the bark beetle outbreak model including the
911 need to update the beetle's phenology model to reflect recent climate changes, and the need to consider extreme
912 drought as a trigger for bark beetle outbreaks in line with emerging evidence. Looking ahead, future work will
913 further develop the capability of ORCHIDEE to simulate interacting disturbances such as the interplay between
914 extreme droughts, storms, and bark beetles, and between storms, bark beetles, and fires.

915

916 The final step will be a quantitative evaluation based on observed data (Marini et al., 2017) in order to assess the
917 capability of ORCHIDEE to simulate complex interaction between multiple sources of tree mortality affecting the
918 carbon balance at large scale.

919

920 **8. Code availability**

921 • R script and data are available at :

922 <https://doi.org/10.5281/zenodo.12806280>

923 • ORCHIDEE rev 7791 code is also available from:

924 https://forge.ipsl.jussieu.fr/orchidee/browser/branches/publications/ORCHIDEE_Bark_beetles_outbreak_g
925 [md_2024](#)

926

927 **9. Data availability**

928 • The Fluxnet climate forcing data are available at <https://fluxnet.org/>

929 • The simulation results use in this study are available at <https://doi.org/10.5281/zenodo.12806280>

930

931

932 **10. Author contribution**

933 G. Marie, S. Luyssaert designed the experiments and G. Marie conducted them. Following discussions with H.

934 Jactel, G. Petter and M. Cailleret, G. Marie developed the bark beetles model code and performed the simulations. J.

935 Jeong integrated the wind damage and bark beetle models with each other. G. Marie, J. Jeong, V. Bastrikov, J.

936 Ghattas, B. Guenet, A.S. Lansø, M.J. McGrath, K. Naudts, A. Valade, C. Yue, and S. Luyssaert, contributed to the

937 development, parameterization and evaluation of the ORCHIDEE revision used in this study. G. Marie, J. Jeong, and

938 S. Luyssaert prepared the manuscript with contributions from all co-authors.

939

940 **11. Competing interests**

941 No competing interest

942

943 12. Acknowledgements

944 GM was funded by MSCF (CLIMPRO) and ADEME (DIPROG). SL and KN were funded by Horizon 2020,
945 HoliSoils (SEP-210673589) and Horizon Europe INFORMA (101060309). JJ and BG were funded by Horizon
946 2020, HoliSoils (SEP-210673589). GP acknowledges funding by the Swiss National Science Foundation (SNF
947 163250). ASL was funded by Horizon 2020, Crescendo (641816). C.Y. was funded by the National Science
948 Foundation of China (U20A2090 and 41971132). MJM was supported by the European Commission, Horizon 2020
949 Framework Programme (VERIFY, grant no. 776810) and the European Union's Horizon 2020 research and
950 innovation programme under Grant Agreement No. 958927 (CoCO2). AV acknowledges funding by Agropolis
951 Fondation (2101-048). This work was performed using HPC resources from GENCI-TGCC (Grant 2022-06328).
952 The Textual AI - Open AI GPT4 (<https://chat.openai.com/>) has been used for language editing at an early stage of
953 manuscript preparation.

954

955 13. References

- 956 Abramowitz, G., Leuning, R., Clark, M., and Pitman, A.: Evaluating the Performance of Land Surface Models, *J.*
957 *Clim.*, 21, 5468–5481, <https://doi.org/10.1175/2008JCLI2378.1>, 2008.
- 958 Allen, C. D., Breshears, D. D., and McDowell, N. G.: On underestimation of global vulnerability to tree mortality
959 and forest die-off from hotter drought in the Anthropocene, *Ecosphere*, 6, art129,
960 <https://doi.org/10.1890/ES15-00203.1>, 2015.
- 961 Andrus, R. A., Hart, S. J., and Veblen, T. T.: Forest recovery following synchronous outbreaks of spruce and western
962 balsam bark beetle is slowed by ungulate browsing, *Ecology*, 101, e02998, <https://doi.org/10.1002/ecy.2998>, 2020.
- 963 Angers, V. A., Drapeau, P., and Bergeron, Y.: Mineralization rates and factors influencing snag decay in four North
964 American boreal tree species, *Can. J. For. Res.*, 42, 157–166, <https://doi.org/10.1139/x11-167>, 2012.
- 965 European State of the Climate | Copernicus: <https://climate.copernicus.eu/ESOTC>, last access: 25 March 2024.
- 966 Bakke, A.: The recent *Ips typographus* outbreak in Norway - experiences from a control program, *Ecography*, 12,
967 515–519, <https://doi.org/10.1111/j.1600-0587.1989.tb00930.x>, 1989.
- 968 Ballard, R. G., Walsh, M. A., and Cole, W. E.: Blue-stain fungi in xylem of lodgepole pine: a light-microscope study
969 on extent of hyphal distribution, *Can. J. Bot.*, 60, 2334–2341, <https://doi.org/10.1139/b82-285>, 1982.
- 970 Bentz, B. J., Régnière, J., Fettig, C. J., Hansen, E. M., Hayes, J. L., Hicke, J. A., Kelsey, R. G., Negrón, J. F., and
971 Seybold, S. J.: Climate Change and Bark Beetles of the Western United States and Canada: Direct and Indirect
972 Effects, *BioScience*, 60, 602–613, <https://doi.org/10.1525/bio.2010.60.8.6>, 2010.
- 973 Berner, L. T., Law, B. E., Meddens, A. J. H., and Hicke, J. A.: Tree mortality from fires, bark beetles, and timber
974 harvest during a hot and dry decade in the western United States (2003–2012), *Environ. Res. Lett.*, 12, 065005,
975 <https://doi.org/10.1088/1748-9326/aa6f94>, 2017.
- 976 Berryman, A. A.: *Population Cycles: The Case for Trophic Interactions*, Oxford University Press, 207 pp., 2002.
- 977 Biedermann, P. H. W., Müller, J., Grégoire, J.-C., Gruppe, A., Hagge, J., Hammerbacher, A., Hofstetter, R. W.,
978 Kandasamy, D., Kolarik, M., Kostovcik, M., Krokene, P., Sallé, A., Six, D. L., Turrini, T., Vanderpool, D.,
979 Wingfield, M. J., and Bässler, C.: Bark Beetle Population Dynamics in the Anthropocene: Challenges and Solutions,
980 *Trends Ecol. Evol.*, 34, 914–924, <https://doi.org/10.1016/j.tree.2019.06.002>, 2019.
- 981 Boucher, O., Servonnat, J., Albright, A. L., Aumont, O., Balkanski, Y., Bastrikov, V., Bekki, S., Bonnet, R., Bony, S.,
982 Bopp, L., Braconnot, P., Brockmann, P., Cadule, P., Caubel, A., Cheruy, F., Codron, F., Cozic, A., Cugnet, D.,
983 D'Andrea, F., Davini, P., Lavergne, C. de, Denvil, S., Deshayes, J., Devilliers, M., Ducharne, A., Dufresne, J.-L.,
984 Dupont, E., Éthé, C., Fairhead, L., Falletti, L., Flavoni, S., Foujols, M.-A., Gardoll, S., Gastineau, G., Ghattas, J.,
985 Grandpeix, J.-Y., Guenet, B., Guez, L., E., Guilyardi, E., Guimberteau, M., Hauglustaine, D., Hourdin, F., Idelkadi,
986 A., Joussaume, S., Kageyama, M., Khodri, M., Krinner, G., Lebas, N., Levvasseur, G., Lévy, C., Li, L., Lott, F.,
987 Lurton, T., Luysaert, S., Madec, G., Madeleine, J.-B., Maignan, F., Marchand, M., Marti, O., Mellul, L.,
988 Meurdesoif, Y., Mignot, J., Musat, I., Ottlé, C., Peylin, P., Planton, Y., Polcher, J., Rio, C., Rochetin, N., Rousset, C.,
989 Sepulchre, P., Sima, A., Swingedouw, D., Thiéblemont, R., Traore, A. K., Vancoppenolle, M., Vial, J., Vialard, J.,
990 Viovy, N., and Vuichard, N.: Presentation and Evaluation of the IPSL-CM6A-LR Climate Model, *J. Adv. Model.*

991 Earth Syst., 12, e2019MS002010, <https://doi.org/10.1029/2019MS002010>, 2020.

992 Bugmann, H. K. M.: A Simplified Forest Model to Study Species Composition Along Climate Gradients, *Ecology*,
993 77, 2055–2074, <https://doi.org/10.2307/2265700>, 1996.

994 Buma, B.: Disturbance interactions: characterization, prediction, and the potential for cascading effects, *Ecosphere*,
995 6, art70, <https://doi.org/10.1890/ES15-00058.1>, 2015.

996 Chen, Y., Ryder, J., Bastrikov, V., McGrath, M. J., Naudts, K., Otto, J., Otlé, C., Peylin, P., Polcher, J., Valade, A.,
997 Black, A., Elbers, J. A., Moors, E., Foken, T., van Gorsel, E., Haverd, V., Heinesch, B., Tiedemann, F., Knohl, A.,
998 Launiainen, S., Loustau, D., Ogée, J., Vessala, T., and Luysaert, S.: Evaluating the performance of land surface
999 model ORCHIDEE-CAN v1.0 on water and energy flux estimation with a single- and multi-layer energy budget
1000 scheme, *Geosci. Model Dev.*, 9, 2951–2972, <https://doi.org/10.5194/gmd-9-2951-2016>, 2016.

1001 Chen, Y.-Y., Gardiner, B., Pasztor, F., Blennow, K., Ryder, J., Valade, A., Naudts, K., Otto, J., McGrath, M. J.,
1002 Planque, C., and Luysaert, S.: Simulating damage for wind storms in the land surface model ORCHIDEE-CAN
1003 (revision 4262), *Geosci. Model Dev.*, 11, 771–791, <https://doi.org/10.5194/gmd-11-771-2018>, 2018.

1004 Ciais, P., Reichstein, M., Viovy, N., Granier, A., Ogée, J., Allard, V., Aubinet, M., Buchmann, N., Bernhofer, C.,
1005 Carrara, A., Chevallier, F., De Noblet, N., Friend, A. D., Friedlingstein, P., Grünwald, T., Heinesch, B., Keronen, P.,
1006 Knohl, A., Krinner, G., Loustau, D., Manca, G., Matteucci, G., Miglietta, F., Ourcival, J. M., Papale, D., Pilegaard,
1007 K., Rambal, S., Seufert, G., Soussana, J. F., Sanz, M. J., Schulze, E. D., Vesala, T., and Valentini, R.: Europe-wide
1008 reduction in primary productivity caused by the heat and drought in 2003, *Nature*, 437, 529–533,
1009 <https://doi.org/10.1038/nature03972>, 2005.

1010 Cox, P. M., Betts, R. A., Jones, C. D., Spall, S. A., and Totterdell, I. J.: Acceleration of global warming due to
1011 carbon-cycle feedbacks in a coupled climate model, *Nature*, 408, 184–187, <https://doi.org/10.1038/35041539>, 2000.

1012 Custer, G. F., van Diepen, L. T. A., and Stump, W. L.: Structural and Functional Dynamics of Soil Microbes
1013 following Spruce Beetle Infestation, *Appl. Environ. Microbiol.*, 86, e01984-19,
1014 <https://doi.org/10.1128/AEM.01984-19>, 2020.

1015 Das, A. J., Stephenson, N. L., and Davis, K. P.: Why do trees die? Characterizing the drivers of background tree
1016 mortality, *Ecology*, 97, 2616–2627, <https://doi.org/10.1002/ecy.1497>, 2016.

1017 Deleuze, C., Pain, O., Dhôte, J.-F., and Hervé, J.-C.: A flexible radial increment model for individual trees in pure
1018 even-aged stands, *Ann. For. Sci.*, 61, 327–335, <https://doi.org/10.1051/forest:2004026>, 2004.

1019 Edburg, S. L., Hicke, J. A., Brooks, P. D., Pendall, E. G., Ewers, B. E., Norton, U., Gochis, D., Gutmann, E. D., and
1020 Meddens, A. J.: Cascading impacts of bark beetle-caused tree mortality on coupled biogeophysical and
1021 biogeochemical processes, *Front. Ecol. Environ.*, 10, 416–424, <https://doi.org/10.1890/110173>, 2012.

1022 Faccoli, M. and Stergulc, F.: A practical method for predicting the short-time trend of bivoltine populations of *Ips*
1023 *typographus* (L.) (Col., Scolytidae), *J. Appl. Entomol.*, 130, 61–66,
1024 <https://doi.org/10.1111/j.1439-0418.2005.01019.x>, 2006.

1025 Friedlingstein, P., Cox, P., Betts, R., Bopp, L., Bloh, W. von, Brovkin, V., Cadule, P., Doney, S., Eby, M., Fung, I.,
1026 Bala, G., John, J., Jones, C., Joos, F., Kato, T., Kawamiya, M., Knorr, W., Lindsay, K., Matthews, H. D., Raddatz, T.,
1027 Rayner, P., Reick, C., Roeckner, E., Schnitzler, K.-G., Schnur, R., Strassmann, K., Weaver, A. J., Yoshikawa, C., and
1028 Zeng, N.: Climate–Carbon Cycle Feedback Analysis: Results from the C4MIP Model Intercomparison, *J. Clim.*, 19,
1029 3337–3353, <https://doi.org/10.1175/JCLI3800.1>, 2006.

1030 Grimm, V. and Wissel, C.: Babel, or the ecological stability discussions: an inventory and analysis of terminology
1031 and a guide for avoiding confusion, *Oecologia*, 109, 323–334, <https://doi.org/10.1007/s004420050090>, 1997.

1032 Havašová, M., Ferenčík, J., and Jakuš, R.: Interactions between windthrow, bark beetles and forest management in
1033 the Tatra national parks, *For. Ecol. Manag.*, 391, 349–361, <https://doi.org/10.1016/j.foreco.2017.01.009>, 2017.

1034 Haverd, V., Lovell, J. L., Cuntz, M., Jupp, D. L. B., Newnham, G. J., and Sea, W.: The Canopy Semi-analytic Pgap
1035 And Radiative Transfer (CanSPART) model: Formulation and application, *Agric. For. Meteorol.*, 160, 14–35,
1036 <https://doi.org/10.1016/j.agrformet.2012.01.018>, 2012.

1037 Hicke, J. A., Allen, C. D., Desai, A. R., Dietze, M. C., Hall, R. J., Hogg, E. H., Kashian, D. M., Moore, D., Raffa, K.
1038 F., Sturrock, R. N., and Vogelmann, J.: Effects of biotic disturbances on forest carbon cycling in the United States
1039 and Canada., <https://doi.org/10.1111/j.1365-2486.2011.02543.x>, 2012.

1040 Hlásny, T., König, L., Krokene, P., Lindner, M., Montagné-Huck, C., Müller, J., Qin, H., Raffa, K. F., Schelhaas,
1041 M.-J., Svoboda, M., Viiri, H., and Seidl, R.: Bark Beetle Outbreaks in Europe: State of Knowledge and Ways
1042 Forward for Management, *Curr. For. Rep.*, 7, 138–165, <https://doi.org/10.1007/s40725-021-00142-x>, 2021a.

1043 Hlásny, T., Zimová, S., Merganičová, K., Štěpánek, P., Modlinger, R., and Turčáni, M.: Devastating outbreak of bark
1044 beetles in the Czech Republic: Drivers, impacts, and management implications, *For. Ecol. Manag.*, 490, 119075,
1045 <https://doi.org/10.1016/j.foreco.2021.119075>, 2021b.

1046 Huang, J., Kautz, M., Trowbridge, A. M., Hammerbacher, A., Raffa, K. F., Adams, H. D., Goodsman, D. W., Xu, C.,

1047 Meddens, A. J. H., Kandasamy, D., Gershenson, J., Seidl, R., and Hartmann, H.: Tree defence and bark beetles in a
1048 drying world: carbon partitioning, functioning and modelling, *New Phytol.*, 225, 26–36,
1049 <https://doi.org/10.1111/nph.16173>, 2020.

1050 Jönsson, A. M., Appelberg, G., Harding, S., and Barring, L.: Spatio-temporal impact of climate change on the
1051 activity and voltinism of the spruce bark beetle, *Ips typographus*, *Glob. Change Biol.*, 15, 486–499,
1052 <https://doi.org/10.1111/j.1365-2486.2008.01742.x>, 2009.

1053 Jönsson, A. M., Harding, S., Krokene, P., Lange, H., Lindelöw, Å., Økland, B., Ravn, H. P., and Schroeder, L. M.:
1054 Modelling the potential impact of global warming on *Ips typographus* voltinism and reproductive diapause, *Clim.*
1055 *Change*, 109, 695–718, <https://doi.org/10.1007/s10584-011-0038-4>, 2011.

1056 Jönsson, A. M., Schroeder, L. M., Lagergren, F., Anderbrant, O., and Smith, B.: Guess the impact of *Ips*
1057 *typographus*—An ecosystem modelling approach for simulating spruce bark beetle outbreaks, *Agric. For. Meteorol.*,
1058 166–167, 188–200, <https://doi.org/10.1016/j.agrformet.2012.07.012>, 2012.

1059 Kärvelo, S. and Schroeder, L. M.: A comparison of outbreak dynamics of the spruce bark beetle in Sweden and the
1060 mountain pine beetle in Canada (Curculionidae: Scolytinae), 2010.

1061 Kautz, M., Anthoni, P., Meddens, A. J. H., Pugh, T. A. M., and Arneeth, A.: Simulating the recent impacts of multiple
1062 biotic disturbances on forest carbon cycling across the United States, *Glob. Change Biol.*, 24, 2079–2092,
1063 <https://doi.org/10.1111/gcb.13974>, 2018.

1064 Komonen, A., Schroeder, L. M., and Weslien, J.: *Ips typographus* population development after a severe storm in a
1065 nature reserve in southern Sweden, *J. Appl. Entomol.*, 135, 132–141,
1066 <https://doi.org/10.1111/j.1439-0418.2010.01520.x>, 2011.

1067 Krinner, G., Viovy, N., de Noblet-Ducoudré, N., Ogée, J., Polcher, J., Friedlingstein, P., Ciais, P., Sitch, S., and
1068 Prentice, I. C.: A dynamic global vegetation model for studies of the coupled atmosphere-biosphere system: DVG
1069 FOR COUPLED CLIMATE STUDIES, *Glob. Biogeochem. Cycles*, 19, <https://doi.org/10.1029/2003GB002199>,
1070 2005.

1071 Kurz, W. A., Dymond, C. C., Stinson, G., Rampley, G. J., Neilson, E. T., Carroll, A. L., Ebata, T., and Safranyik, L.:
1072 Mountain pine beetle and forest carbon feedback to climate change, *Nature*, 452, 987–990,
1073 <https://doi.org/10.1038/nature06777>, 2008a.

1074 Kurz, W. A., Dymond, C. C., Stinson, G., Rampley, G. J., Neilson, E. T., Carroll, A. L., Ebata, T., and Safranyik, L.:
1075 Mountain pine beetle and forest carbon feedback to climate change, *Nature*, 452, 987–990,
1076 <https://doi.org/10.1038/nature06777>, 2008b.

1077 Kurz, W. A., Stinson, G., Rampley, G. J., Dymond, C. C., and Neilson, E. T.: Risk of natural disturbances makes
1078 future contribution of Canada’s forests to the global carbon cycle highly uncertain, *Proc. Natl. Acad. Sci.*, 105,
1079 1551–1555, <https://doi.org/10.1073/pnas.0708133105>, 2008c.

1080 Lasslop, G., Thonicke, K., and Kloster, S.: SPITFIRE within the MPI Earth system model: Model development and
1081 evaluation, *J. Adv. Model. Earth Syst.*, 6, 740–755, <https://doi.org/10.1002/2013MS000284>, 2014.

1082 Lausch, A., Fahse, L., and Heurich, M.: Factors affecting the spatio-temporal dispersion of *Ips typographus* (L.) in
1083 Bavarian Forest National Park: A long-term quantitative landscape-level analysis, *For. Ecol. Manag.*, 261, 233–245,
1084 <https://doi.org/10.1016/j.foreco.2010.10.012>, 2011.

1085 Levins, R.: The Strategy of Model Building in Population Biology, *Am. Sci.*, 54, 421–431, 1966.

1086 Lieutier, F.: Mechanisms of Resistance in Conifers and Bark beetle Attack Strategies, in: *Mechanisms and*
1087 *Deployment of Resistance in Trees to Insects*, edited by: Wagner, M. R., Clancy, K. M., Lieutier, F., and Paine, T. D.,
1088 Springer Netherlands, Dordrecht, 31–77, https://doi.org/10.1007/0-306-47596-0_2, 2002.

1089 Lombardero, M. J., Ayres, M. P., Ayres, B. D., and Reeve, J. D.: Cold Tolerance of Four Species of Bark Beetle
1090 (Coleoptera: Scolytidae) in North America, *Environ. Entomol.*, 29, 421–432,
1091 <https://doi.org/10.1603/0046-225X-29.3.421>, 2000.

1092 Luyssaert, S., Marie, G., Valade, A., Chen, Y.-Y., Njakou Djomo, S., Ryder, J., Otto, J., Naudts, K., Lansø, A. S.,
1093 Ghattas, J., and McGrath, M. J.: Trade-offs in using European forests to meet climate objectives, *Nature*, 562,
1094 259–262, <https://doi.org/10.1038/s41586-018-0577-1>, 2018.

1095 Marini, L., Økland, B., Jönsson, A. M., Bentz, B., Carroll, A., Forster, B., Grégoire, J.-C., Hurling, R., Nageleisen,
1096 L. M., Netherer, S., Ravn, H. P., Weed, A., and Schroeder, M.: Climate drivers of bark beetle outbreak dynamics in
1097 Norway spruce forests, *Ecography*, 40, 1426–1435, <https://doi.org/10.1111/ecog.02769>, 2017.

1098 Mezei, P., Grodzki, W., Blaženec, M., and Jakuš, R.: Factors influencing the *wind-bark beetles*’ disturbance system
1099 in the course of an *Ips typographus* outbreak in the Tatra Mountains, *For. Ecol. Manag.*, 312, 67–77,
1100 <https://doi.org/10.1016/j.foreco.2013.10.020>, 2014.

1101 Mezei, P., Jakuš, R., Pennerstorfer, J., Havašová, M., Škvarenina, J., Ferenčík, J., Slivinský, J., Bičárová, S., Bilčík,
1102 D., Blaženec, M., and Netherer, S.: Storms, temperature maxima and the Eurasian spruce bark beetle *Ips*

1103 *typographus*—An infernal trio in Norway spruce forests of the Central European High Tatra Mountains, *Agric. For.*
1104 *Meteorol.*, 242, 85–95, <https://doi.org/10.1016/j.agrformet.2017.04.004>, 2017.

1105 Migliavacca, M., Dosio, A., Kloster, S., Ward, D. S., Camia, A., Houborg, R., Houston Durrant, T., Khabarov, N.,
1106 Krasovskii, A. A., San Miguel-Ayanz, J., and Cescatti, A.: Modeling burned area in Europe with the Community
1107 Land Model, *J. Geophys. Res. Biogeosciences*, 118, 265–279, <https://doi.org/10.1002/jgrg.20026>, 2013.

1108 Migliavacca, M., Musavi, T., Mahecha, M. D., Nelson, J. A., Knauer, J., Baldocchi, D. D., Perez-Priego, O.,
1109 Christiansen, R., Peters, J., Anderson, K., Bahn, M., Black, T. A., Blanken, P. D., Bonal, D., Buchmann, N.,
1110 Caldararu, S., Carrara, A., Carvalhais, N., Cescatti, A., Chen, J., Cleverly, J., Cremonese, E., Desai, A. R.,
1111 El-Madany, T. S., Farella, M. M., Fernández-Martínez, M., Filippa, G., Forkel, M., Galvagno, M., Gomasasca, U.,
1112 Gough, C. M., Göckede, M., Ibrom, A., Ikawa, H., Janssens, I. A., Jung, M., Kattge, J., Keenan, T. F., Knohl, A.,
1113 Kobayashi, H., Kraemer, G., Law, B. E., Liddell, M. J., Ma, X., Mammarella, I., Martini, D., Macfarlane, C.,
1114 Matteucci, G., Montagnani, L., Pabon-Moreno, D. E., Panigada, C., Papale, D., Pendall, E., Penuelas, J., Phillips, R.
1115 P., Reich, P. B., Rossini, M., Rotenberg, E., Scott, R. L., Stahl, C., Weber, U., Wohlfahrt, G., Wolf, S., Wright, I. J.,
1116 Yakir, D., Zaehle, S., and Reichstein, M.: The three major axes of terrestrial ecosystem function, *Nature*, 598,
1117 468–472, <https://doi.org/10.1038/s41586-021-03939-9>, 2021.

1118 Millar, C. I. and Stephenson, N. L.: Temperate forest health in an era of emerging megadisturbance, *Science*, 349,
1119 823–826, <https://doi.org/10.1126/science.aaa9933>, 2015.

1120 Morehouse, K., Johns, T., Kaye, J., and Kaye, M.: Carbon and nitrogen cycling immediately following bark beetle
1121 outbreaks in southwestern ponderosa pine forests, *For. Ecol. Manag.*, 255, 2698–2708,
1122 <https://doi.org/10.1016/j.foreco.2008.01.050>, 2008.

1123 Nardi, D., Jactel, H., Pagot, E., Samalens, J.-C., and Marini, L.: Drought and stand susceptibility to attacks by the
1124 European spruce bark beetle: A remote sensing approach, *Agric. For. Entomol.*, 25, 119–129,
1125 <https://doi.org/10.1111/afe.12536>, 2023.

1126 Naudts, K., Ryder, J., McGrath, M. J., Otto, J., Chen, Y., Valade, A., Bellasen, V., Berhongaray, G., Bönisch, G.,
1127 Campioli, M., and others: A vertically discretised canopy description for ORCHIDEE (SVN r2290) and the
1128 modifications to the energy, water and carbon fluxes, *Geosci. Model Dev.*, 8, 2035–2065, 2015a.

1129 Naudts, K., Ryder, J., McGrath, M. J., Otto, J., Chen, Y., Valade, A., Bellasen, V., Berhongaray, G., Bönisch, G.,
1130 Campioli, M., Ghattas, J., De Groot, T., Haverd, V., Kattge, J., MacBean, N., Maignan, F., Merilä, P., Penuelas, J.,
1131 Peylin, P., Pinty, B., Pretzsch, H., Schulze, E. D., Solyga, D., Vuichard, N., Yan, Y., and Luysaert, S.: A vertically
1132 discretised canopy description for ORCHIDEE (SVN r2290) and the modifications to the energy, water and carbon
1133 fluxes, *Geosci. Model Dev.*, 8, 2035–2065, <https://doi.org/10.5194/gmd-8-2035-2015>, 2015b.

1134 Naudts, K., Chen, Y., McGrath, M. J., Ryder, J., Valade, A., Otto, J., and Luysaert, S.: Europe’s forest management
1135 did not mitigate climate warming, *Science*, 351, 597–600, <https://doi.org/10.1126/science.aad7270>, 2016.

1136 Netherer, S., Matthews, B., Katzensteiner, K., Blackwell, E., Henschke, P., Hietz, P., Pennerstorfer, J., Rosner, S.,
1137 Kikuta, S., Schume, H., and Schopf, A.: Do water-limiting conditions predispose Norway spruce to bark beetle
1138 attack?, *New Phytol.*, 205, 1128–1141, <https://doi.org/10.1111/nph.13166>, 2015.

1139 Ogris, N., Ferlan, M., Hauptman, T., Pavlin, R., Kavčič, A., Jurc, M., and de Groot, M.: RITY – A phenology model
1140 of *Ips typographus* as a tool for optimization of its monitoring, *Ecol. Model.*, 410, 108775,
1141 <https://doi.org/10.1016/j.ecolmodel.2019.108775>, 2019.

1142 Pastorello, G., Trotta, C., Canfora, E., Chu, H., Christianson, D., Cheah, Y.-W., Poindexter, C., Chen, J., Elbashandy,
1143 A., Humphrey, M., Isaac, P., Polidori, D., Reichstein, M., Ribeca, A., van Ingen, C., Vuichard, N., Zhang, L., Amiro,
1144 B., Ammann, C., Arain, M. A., Ardö, J., Arkebauer, T., Arndt, S. K., Arriga, N., Aubinet, M., Aurela, M., Baldocchi,
1145 D., Barr, A., Beamesderfer, E., Marchesini, L. B., Bergeron, O., Beringer, J., Bernhofer, C., Berveiller, D.,
1146 Billesbach, D., Black, T. A., Blanken, P. D., Bohrer, G., Boike, J., Bolstad, P. V., Bonal, D., Bonnefond, J.-M.,
1147 Bowling, D. R., Bracho, R., Brodeur, J., Brümmer, C., Buchmann, N., Burban, B., Burns, S. P., Buysse, P., Cale, P.,
1148 Cavagna, M., Cellier, P., Chen, S., Chini, I., Christensen, T. R., Cleverly, J., Collalti, A., Consalvo, C., Cook, B. D.,
1149 Cook, D., Coursolle, C., Cremonese, E., Curtis, P. S., D’Andrea, E., da Rocha, H., Dai, X., Davis, K. J., Cinti, B. D.,
1150 Grandcourt, A. de, Ligne, A. D., De Oliveira, R. C., Delpierre, N., Desai, A. R., Di Bella, C. M., Tommasi, P. di,
1151 Dolman, H., Domingo, F., Dong, G., Dore, S., Duce, P., Dufrêne, E., Dunn, A., Dušek, J., Eamus, D., Eichelmann,
1152 U., ElKhidir, H. A. M., Eugster, W., Ewenz, C. M., Ewers, B., Famulari, D., Fares, S., Feigenwinter, I., Feitz, A.,
1153 Fensholt, R., Filippa, G., Fischer, M., Frank, J., Galvagno, M., et al.: The FLUXNET2015 dataset and the ONEFlux
1154 processing pipeline for eddy covariance data, *Sci. Data*, 7, 225, <https://doi.org/10.1038/s41597-020-0534-3>, 2020.

1155 Pasztor, F., Matulla, C., Rammer, W., and Lexer, M. J.: Drivers of the bark beetle disturbance regime in Alpine
1156 forests in Austria, *For. Ecol. Manag.*, 318, 349–358, <https://doi.org/10.1016/j.foreco.2014.01.044>, 2014.

1157 Pfeifer, E. M., Hicke, J. A., and Meddens, A. J. H.: Observations and modeling of aboveground tree carbon stocks
1158 and fluxes following a bark beetle outbreak in the western United States, *Glob. Change Biol.*, 17, 339–350,

1159 <https://doi.org/10.1111/j.1365-2486.2010.02226.x>, 2011.

1160 Pineau, X., David, G., Peter, Z., Sallé, A., Baude, M., Lieutier, F., and Jactel, H.: Effect of temperature on the
1161 reproductive success, developmental rate and brood characteristics of *Ips sexdentatus* (Boern.), *Agric. For. Entomol.*,
1162 19, 23–33, <https://doi.org/10.1111/afe.12177>, 2017.

1163 Preisler, H. K., Hicke, J. A., Ager, A. A., and Hayes, J. L.: Climate and weather influences on spatial temporal
1164 patterns of mountain pine beetle populations in Washington and Oregon, *Ecology*, 93, 2421–2434,
1165 <https://doi.org/10.1890/11-1412.1>, 2012.

1166 Pugh, T. A. M., Jones, C. D., Huntingford, C., Burton, C., Arneith, A., Brovkin, V., Ciais, P., Lomas, M., Robertson,
1167 E., and Piao, S. L.: A Large Committed Long-Term Sink of Carbon due to Vegetation Dynamics, *Earths Future*,
1168 2017.

1169 Quillet, A., Peng, C., and Garneau, M.: Toward dynamic global vegetation models for simulating vegetation–climate
1170 interactions and feedbacks: recent developments, limitations, and future challenges, *Environ. Rev.*, 18, 333–353,
1171 <https://doi.org/10.1139/A10-016>, 2010.

1172 Raffa, K. F., Aukema, B. H., Bentz, B. J., Carroll, A. L., Hicke, J. A., Turner, M. G., and Romme, W. H.: Cross-scale
1173 Drivers of Natural Disturbances Prone to Anthropogenic Amplification: The Dynamics of Bark Beetle Eruptions,
1174 *BioScience*, 58, 501–517, <https://doi.org/10.1641/B580607>, 2008.

1175 Ryder, J., Polcher, J., Peylin, P., Ottlé, C., Chen, Y., van Gorsel, E., Haverd, V., McGrath, M. J., Naudds, K., Otto, J.,
1176 Valade, A., and Luysaert, S.: A multi-layer land surface energy budget model for implicit coupling with global
1177 atmospheric simulations, *Geosci. Model Dev.*, 9, 223–245, <https://doi.org/10.5194/gmd-9-223-2016>, 2016.

1178 Schumacher, S.: The role of large-scale disturbances and climate for the dynamics of forested landscapes in the
1179 European Alps, Doctoral Thesis, ETH Zurich, <https://doi.org/10.3929/ethz-a-004818825>, 2004.

1180 Seidl, R. and Rammer, W.: Climate change amplifies the interactions between wind and bark beetle disturbances in
1181 forest landscapes, *Landsc. Ecol.*, 1–14, <https://doi.org/10.1007/s10980-016-0396-4>, 2016.

1182 Seidl, R., Fernandes, P. M., Fonseca, T. F., Gillet, F., Jönsson, A. M., Merganičová, K., Netherer, S., Arpaci, A.,
1183 Bontemps, J.-D., Bugmann, H., González-Olabarria, J. R., Lasch, P., Meredieu, C., Moreira, F., Schelhaas, M.-J., and
1184 Mohren, F.: Modelling natural disturbances in forest ecosystems: a review, *Ecol. Model.*, 222, 903–924,
1185 <https://doi.org/10.1016/j.ecolmodel.2010.09.040>, 2011.

1186 Seidl, R., Schelhaas, M.-J., Rammer, W., and Verkerk, P. J.: Increasing forest disturbances in Europe and their impact
1187 on carbon storage, *Nat. Clim. Change*, 4, 806–810, <https://doi.org/10.1038/nclimate2318>, 2014.

1188 Seidl, R., Thom, D., Kautz, M., Martin-Benito, D., Peltoniemi, M., Vacchiano, G., Wild, J., Ascoli, D., Petr, M.,
1189 Honkaniemi, J., Lexer, M. J., Trotsiuk, V., Mairota, P., Svoboda, M., Fabrika, M., Nagel, T. A., and Reyer, C. P. O.:
1190 Forest disturbances under climate change, *Nat. Clim. Change*, 7, 395–402, <https://doi.org/10.1038/nclimate3303>,
1191 2017.

1192 Seidl, R., Klöner, G., Rammer, W., Essl, F., Moreno, A., Neumann, M., and Dullinger, S.: Invasive alien pests
1193 threaten the carbon stored in Europe’s forests, *Nat. Commun.*, 9, 1626, <https://doi.org/10.1038/s41467-018-04096-w>,
1194 2018.

1195 Senf, C., Pflugmacher, D., Hostert, P., and Seidl, R.: Using Landsat time series for characterizing forest disturbance
1196 dynamics in the coupled human and natural systems of Central Europe, *ISPRS J. Photogramm. Remote Sens.*, 130,
1197 453–463, <https://doi.org/10.1016/j.isprsjprs.2017.07.004>, 2017.

1198 Storaunet, K. O., Rolstad, J., Gjerde, I., and Gundersen, V. S.: Historical logging, productivity, and structural
1199 characteristics of boreal coniferous forests in Norway, *Silva Fenn.*, 39, 2005.

1200 Temperli, C., Bugmann, H., and Elkin, C.: Cross-scale interactions among bark beetles, climate change, and wind
1201 disturbances: a landscape modeling approach, *Ecol. Monogr.*, 83, 383–402, <https://doi.org/10.1890/12-1503.1>,
1202 2013a.

1203 Temperli, C., Bugmann, H., and Elkin, C.: Cross-scale interactions among bark beetles, climate change, and wind
1204 disturbances: a landscape modeling approach, *Ecol. Monogr.*, 83, 383–402, <https://doi.org/10.1890/12-1503.1>,
1205 2013b.

1206 Thurner, M., Beer, C., Ciais, P., Friend, A. D., Ito, A., Kleidon, A., Lomas, M. R., Quegan, S., Rademacher, T. T.,
1207 Schaphoff, S., Tum, M., Wiltshire, A., and Carvalhais, N.: Evaluation of climate-related carbon turnover processes in
1208 global vegetation models for boreal and temperate forests, *Glob. Change Biol.*, 23, 3076–3091,
1209 <https://doi.org/10.1111/gcb.13660>, 2017.

1210 Van Meerbeek, K., Jucker, T., and Svenning, J.-C.: Unifying the concepts of stability and resilience in ecology, *J.*
1211 *Ecol.*, 109, 3114–3132, <https://doi.org/10.1111/1365-2745.13651>, 2021.

1212 Vuichard, N., Messina, P., Luysaert, S., Guenet, B., Zaehle, S., Ghattas, J., Bastrikov, V., and Peylin, P.: Accounting
1213 for carbon and nitrogen interactions in the global terrestrial ecosystem model ORCHIDEE (trunk version, rev 4999):
1214 multi-scale evaluation of gross primary production, *Geosci. Model Dev.*, 12, 4751–4779,

1215 <https://doi.org/10.5194/gmd-12-4751-2019>, 2019.

1216 Wermelinger, B.: Ecology and management of the spruce bark beetle *Ips typographus*—a review of recent research,
1217 *For. Ecol. Manag.*, 202, 67–82, <https://doi.org/10.1016/j.foreco.2004.07.018>, 2004.

1218 Wichmann, L. and Ravn, H. P.: The spread of *Ips typographus* (L.) (Coleoptera, Scolytidae) attacks following heavy
1219 windthrow in Denmark, analysed using GIS, *For. Ecol. Manag.*, 148, 31–39,
1220 [https://doi.org/10.1016/S0378-1127\(00\)00477-1](https://doi.org/10.1016/S0378-1127(00)00477-1), 2001.

1221 Yao, Y., Joetzjer, E., Ciais, P., Viovy, N., Cresto Aleina, F., Chave, J., Sack, L., Bartlett, M., Meir, P., Fisher, R., and
1222 Luyssaert, S.: Forest fluxes and mortality response to drought: model description (ORCHIDEE-CAN-NHA r7236)
1223 and evaluation at the Caxiuana drought experiment, *Geosci. Model Dev.*, 15, 7809–7833,
1224 <https://doi.org/10.5194/gmd-15-7809-2022>, 2022.

1225 Yi-Ying, C., Gardiner, B., Pasztor, F., Blennow, K., Ryder, J., Valade, A., Naudts, K., Otto, J., McGrath, M. J., and
1226 Planque, C.: Simulating damage for wind storms in the land surface model ORCHIDEE-CAN (revision 4262),
1227 *Geosci. Model Dev.*, 11, 771, 2018.


1228 Yue, C., Ciais, P., Cadule, P., Thonicke, K., Archibald, S., Poulter, B., Hao, W. M., Hantson, S., Mouillot, F.,
1229 Friedlingstein, P., Maignan, F., and Viovy, N.: Modelling the role of fires in the terrestrial carbon balance by
1230 incorporating SPITFIRE into the global vegetation model ORCHIDEE – Part 1: simulating historical global burned
1231 area and fire regimes, *Geosci. Model Dev.*, 7, 2747–2767, <https://doi.org/10.5194/gmd-7-2747-2014>, 2014.


1232 Zaehle, S. and Dalmonech, D.: Carbon–nitrogen interactions on land at global scales: current understanding in
1233 modelling climate biosphere feedbacks, *Curr. Opin. Environ. Sustain.*, 3, 311–320,
1234 <https://doi.org/10.1016/j.cosust.2011.08.008>, 2011.


1235 Zaehle, S. and Friend, A. D.: Carbon and nitrogen cycle dynamics in the O-CN land surface model: 1. Model
1236 description, site-scale evaluation, and sensitivity to parameter estimates, *Glob. Biogeochem. Cycles*, 24,
1237 <https://doi.org/10.1029/2009GB003521>, 2010.


1238 Zhang, Q.-H. and Schlyter, F.: Olfactory recognition and behavioural avoidance of angiosperm nonhost volatiles by
1239 conifer-inhabiting bark beetles, *Agric. For. Entomol.*, 6, 1–20, <https://doi.org/10.1111/j.1461-9555.2004.00202.x>,
1240 2004.


1241 Zscheischler, J., Westra, S., van den Hurk, B. J. J. M., Seneviratne, S. I., Ward, P. J., Pitman, A., AghaKouchak, A.,
1242 Bresch, D. N., Leonard, M., Wahl, T., and Zhang, X.: Future climate risk from compound events, *Nat. Clim. Change*,
1243 8, 469–477, <https://doi.org/10.1038/s41558-018-0156-3>, 2018.


1244 


1245 


1246 


1247 


1248 


1249 


1250 


1251 

1252 

1253 

1254 

1255 

1256 

1257 ¶

1258 ¶

1259 ¶

1260 **Supplementary material:** ¶

Table s1: selection of 32 parameter sets used to assess the sensitivity of four main equations driving the ipstypographus outbreak model. Black values are reference values whereas red values correspond to the sensitivity analysis described in section 3.3. The parameter set in green corresponds to the chosen parameter values for which the credibility score = 4 and the parameter set in green bold is the one chosen for this study. ¶

<i>i</i> _{beetles generation} ¶									
¶	<i>S</i> _{generation} ¶	<i>G</i> _{limit} ¶	<i>S</i> _{activity} ¶	<i>act</i> _{limit} ¶	<i>S</i> _{susceptibility} ¶	<i>i</i> _{rd susceptibility} ¶	<i>S</i> _{mass attack} ¶	<i>BP</i> _{limit} ¶	Score ¶
Set 1.1 ¶	1.0 ¶	0.5 ¶	-20.0 ¶	0.06 ¶	-5.0 ¶	0.55 ¶	-30.0 ¶	0.12 ¶	4 ¶
Set 1.2 ¶	5.0 ¶	0.5 ¶	-20.0 ¶	0.06 ¶	-5.0 ¶	0.55 ¶	-30.0 ¶	0.12 ¶	2 ¶
Set 1.3 ¶	500.0 ¶	0.5 ¶	-20.0 ¶	0.06 ¶	-5.0 ¶	0.55 ¶	-30.0 ¶	0.12 ¶	2 ¶
Set 1.4 ¶	1.0 ¶	1.0 ¶	-20.0 ¶	0.06 ¶	-5.0 ¶	0.55 ¶	-30.0 ¶	0.12 ¶	4 ¶
Set 1.5 ¶	5.0 ¶	1.0 ¶	-20.0 ¶	0.06 ¶	-5.0 ¶	0.55 ¶	-30.0 ¶	0.12 ¶	4 ¶
Set 1.6 ¶	500.0 ¶	1.0 ¶	-20.0 ¶	0.06 ¶	-5.0 ¶	0.55 ¶	-30.0 ¶	0.12 ¶	2 ¶
Set 1.7 ¶	1.0 ¶	1.5 ¶	-20.0 ¶	0.06 ¶	-5.0 ¶	0.55 ¶	-30.0 ¶	0.12 ¶	3 ¶
Set 1.8 ¶	5.0 ¶	1.5 ¶	-20.0 ¶	0.06 ¶	-5.0 ¶	0.55 ¶	-30.0 ¶	0.12 ¶	0 ¶
Set 1.9 ¶	500.0 ¶	1.5 ¶	-20.0 ¶	0.06 ¶	-5.0 ¶	0.55 ¶	-30.0 ¶	0.12 ¶	0 ¶
<i>i</i> _{beetles activity} ¶									
¶	<i>S</i> _{generation} ¶	<i>G</i> _{limit} ¶	<i>S</i> _{activity} ¶	<i>act</i> _{limit} ¶	<i>S</i> _{susceptibility} ¶	<i>i</i> _{rd susceptibility} ¶	<i>S</i> _{mass attack} ¶	<i>BP</i> _{limit} ¶	Score ¶
Set 2.1 ¶	1.0 ¶	1.0 ¶	-1.0 ¶	0.03 ¶	-5.0 ¶	0.55 ¶	-30.0 ¶	0.12 ¶	0 ¶
Set 2.2 ¶	1.0 ¶	1.0 ¶	-20.0 ¶	0.03 ¶	-5.0 ¶	0.55 ¶	-30.0 ¶	0.12 ¶	0 ¶
Set 2.3 ¶	1.0 ¶	1.0 ¶	-500.0 ¶	0.03 ¶	-5.0 ¶	0.55 ¶	-30.0 ¶	0.12 ¶	3 ¶
Set 2.4 ¶	1.0 ¶	1.0 ¶	-1.0 ¶	0.06 ¶	-5.0 ¶	0.55 ¶	-30.0 ¶	0.12 ¶	0 ¶
Set 2.5 ¶	1.0 ¶	1.0 ¶	-20.0 ¶	0.06 ¶	-5.0 ¶	0.55 ¶	-30.0 ¶	0.12 ¶	2 ¶
Set 2.6 ¶	1.0 ¶	1.0 ¶	-500.0 ¶	0.06 ¶	-5.0 ¶	0.55 ¶	-30.0 ¶	0.12 ¶	4 ¶
Set 2.7 ¶	1.0 ¶	1.0 ¶	-1.0 ¶	0.09 ¶	-5.0 ¶	0.55 ¶	-30.0 ¶	0.12 ¶	0 ¶
Set 2.8 ¶	1.0 ¶	1.0 ¶	-20.0 ¶	0.09 ¶	-5.0 ¶	0.55 ¶	-30.0 ¶	0.12 ¶	0 ¶
Set 2.9 ¶	1.0 ¶	1.0 ¶	-500.0 ¶	0.09 ¶	-5.0 ¶	0.55 ¶	-30.0 ¶	0.12 ¶	2 ¶
<i>i</i> _{hosts susceptibility} ¶									
¶	<i>S</i> _{generation} ¶	<i>G</i> _{limit} ¶	<i>S</i> _{activity} ¶	<i>act</i> _{limit} ¶	<i>S</i> _{susceptibility} ¶	<i>i</i> _{rd susceptibility} ¶	<i>S</i> _{mass attack} ¶	<i>BP</i> _{limit} ¶	Score ¶
Set 3.1 ¶	1.0 ¶	1.0 ¶	-20.0 ¶	0.06 ¶	-1.0 ¶	0.275 ¶	-30.0 ¶	0.12 ¶	0 ¶
Set 3.2 ¶	1.0 ¶	1.0 ¶	-20.0 ¶	0.06 ¶	-5.0 ¶	0.275 ¶	-30.0 ¶	0.12 ¶	1 ¶
Set 3.3 ¶	1.0 ¶	1.0 ¶	-20.0 ¶	0.06 ¶	-500.0 ¶	0.275 ¶	-30.0 ¶	0.12 ¶	1 ¶
Set 3.4 ¶	1.0 ¶	1.0 ¶	-20.0 ¶	0.06 ¶	-1.0 ¶	0.55 ¶	-30.0 ¶	0.12 ¶	0 ¶
Set 3.5 ¶	1.0 ¶	1.0 ¶	-20.0 ¶	0.06 ¶	-5.0 ¶	0.55 ¶	-30.0 ¶	0.12 ¶	4 ¶
Set 3.6 ¶	1.0 ¶	1.0 ¶	-20.0 ¶	0.06 ¶	-500.0 ¶	0.55 ¶	-30.0 ¶	0.12 ¶	2 ¶
Set 3.7 ¶	1.0 ¶	1.0 ¶	-20.0 ¶	0.06 ¶	-1.0 ¶	0.825 ¶	-30.0 ¶	0.12 ¶	0 ¶
Set 3.8 ¶	1.0 ¶	1.0 ¶	-20.0 ¶	0.06 ¶	-5.0 ¶	0.825 ¶	-30.0 ¶	0.12 ¶	2 ¶
Set 3.9 ¶	1.0 ¶	1.0 ¶	-20.0 ¶	0.06 ¶	-500.0 ¶	0.825 ¶	-30.0 ¶	0.12 ¶	2 ¶
<i>i</i> _{beetles mass attack} ¶									
¶	<i>S</i> _{generation} ¶	<i>G</i> _{limit} ¶	<i>S</i> _{activity} ¶	<i>act</i> _{limit} ¶	<i>S</i> _{susceptibility} ¶	<i>i</i> _{rd susceptibility} ¶	<i>S</i> _{mass attack} ¶	<i>BP</i> _{limit} ¶	Score ¶

Set 4.1	1.0	1.0	-20.0	0.06	-5.0	0.55	-1.0	0.06	0
Set 4.2	1.0	1.0	-20.0	0.06	-5.0	0.55	-30.0	0.06	0
Set 4.3	1.0	1.0	-20.0	0.06	-5.0	0.55	-500.0	0.06	3
Set 4.4	1.0	1.0	-20.0	0.06	-5.0	0.55	-1.0	0.12	0
Set 4.5	1.0	1.0	-20.0	0.06	-5.0	0.55	-30.0	0.12	4
Set 4.6	1.0	1.0	-20.0	0.06	-5.0	0.55	-500.0	0.12	4
Set 4.7	1.0	1.0	-20.0	0.06	-5.0	0.55	-1.0	0.18	2
Set 4.8	1.0	1.0	-20.0	0.06	-5.0	0.55	-30.0	0.18	3
Set 4.9	1.0	1.0	-20.0	0.06	-5.0	0.55	-500.0	0.18	4

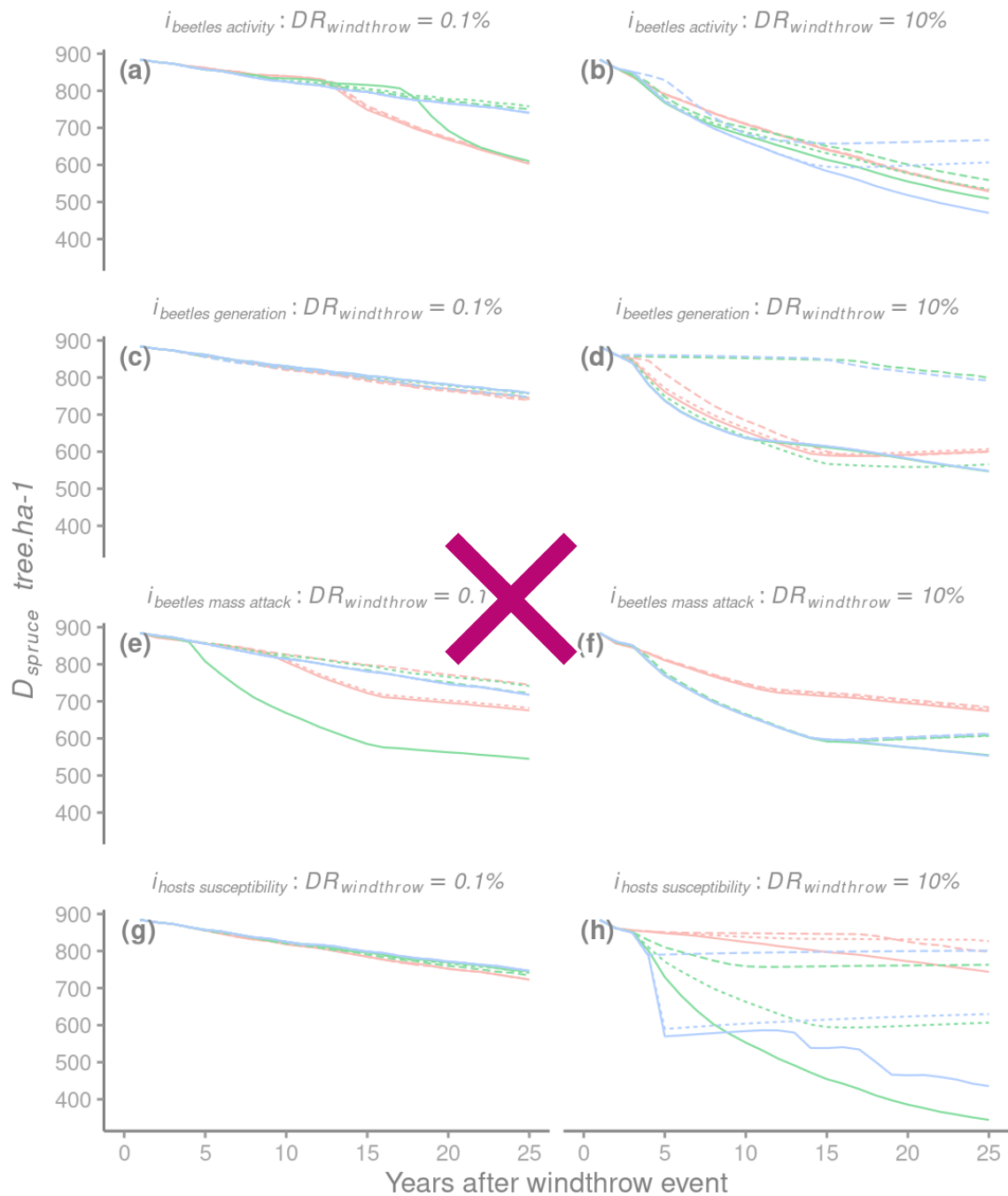
1261

1262

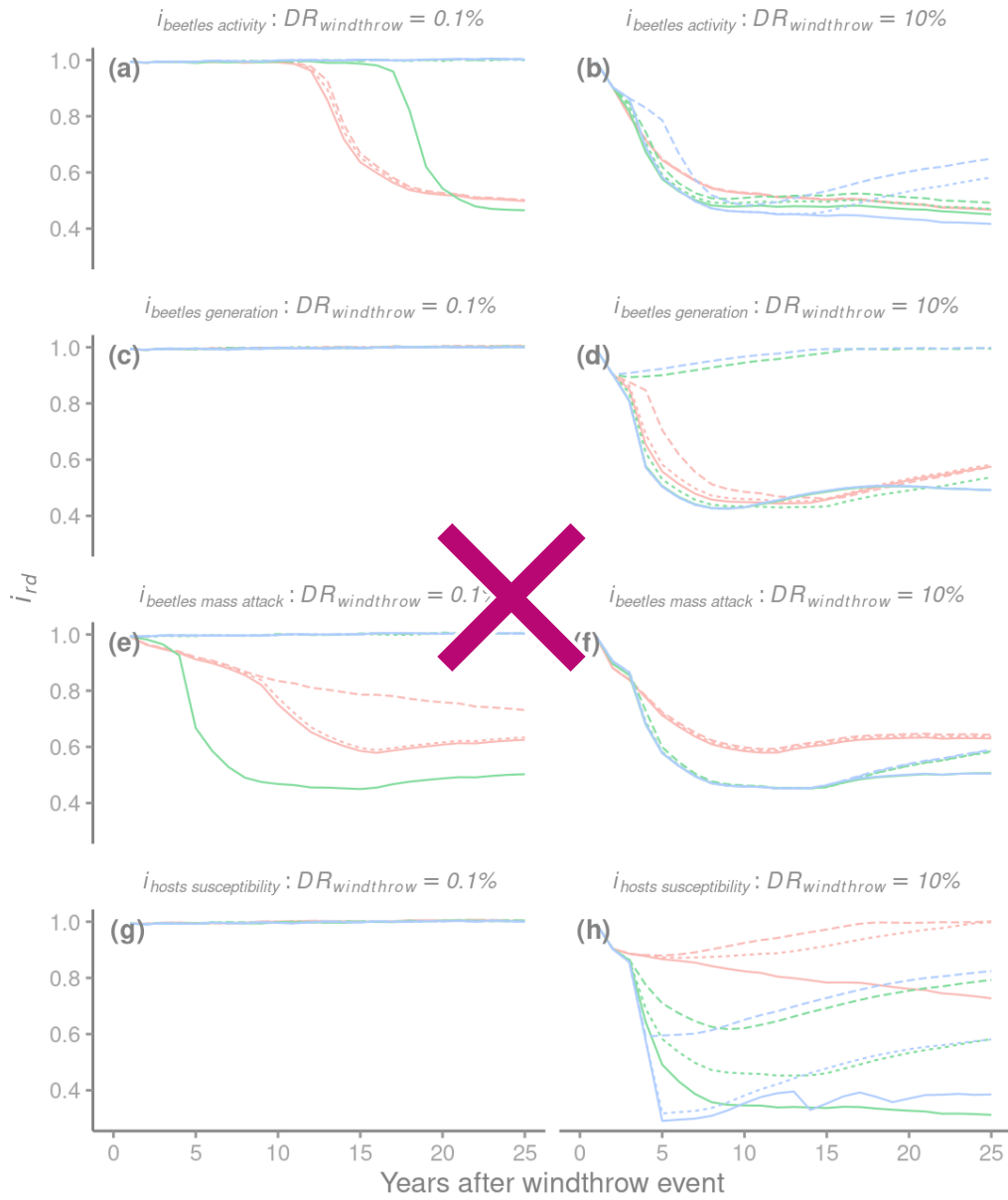
1263

1264

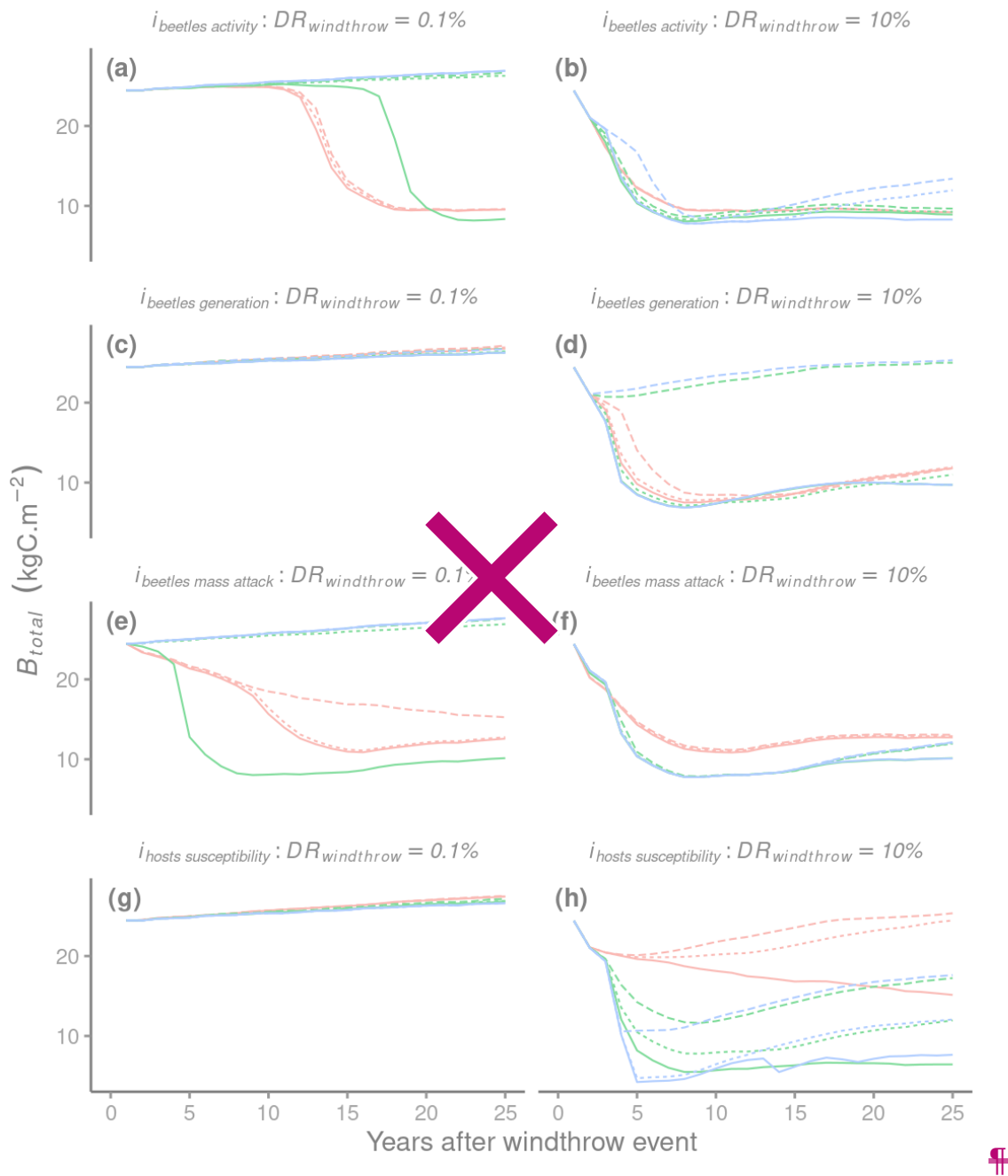
1265



~~Figure s2: Simulation results from the sensitivity experiment at the THA site. Eight parameters from four equations were evaluated. Each equation represents an index from the bark beetle outbreak model (i_{hosts} susceptibility, i_{hosts} mass attack, $i_{beetles}$ activity, $i_{beetles}$ generation). Each index is represented by a logistic function defined by a shape parameter ($Shape$) and a limit parameter ($Limit$). Three values were chosen for each parameter resulting in 9 pairs of parameters for each index. Colored lines represent the shape parameter varying from linear: $Shape = -1.0$ (red), logistic $-5.0 < Shape < -30.0$ (green), to step function where $Shape = 500.0$ (blue). Line type represents three different values for $Limit$ parameters where references (dashed line) are values of i_{hosts} susceptibility, BP_{limb} , act_{limit} and G_{limit} (given in table 4), whereas permissive (full line) and restrictive (dashed dotted) represent a 50% decrease or increase respectively.~~



~~Figure s3. Simulation results from the sensitivity experiment at the THA site. Eight parameters from four equations were evaluated. Each equation represents an index from the bark beetle outbreak model ($i_{\text{hosts susceptibility}}$, $i_{\text{hosts mass attack}}$, $i_{\text{beetles activity}}$, $i_{\text{beetles generation}}$). Each index is represented by a logistic function defined by a shape parameter (*Shape*) and a limit parameter (*Limit*). Three values were chosen for each parameter resulting in 9 pairs of parameters for each index. Colored lines represent the shape parameter varying from linear: $Shape = 1.0$ (red), logistic $5.0 < Shape < 30.0$ (green), to step function where $Shape = 500.0$ (blue). Line type represents three different values for *Limit* parameters where references (dashed line) are values of $i_{\text{rd susceptibility}}$, $BP_{\text{limp act limit}}$ and G_{limit} (given in table 4), whereas permissive (full line) and restrictive (dashed dotted) represent a 50% decrease or increase respectively.~~



~~Figure s4: Simulation results from the sensitivity experiment at the THA site. Eight parameters from four equations were evaluated. Each equation represents an index from the bark beetle outbreak model ($i_{\text{hosts susceptibility}}$, $i_{\text{hosts mass attack}}$, $i_{\text{beetles activity}}$, $i_{\text{beetles generation}}$). Each index is represented by a logistic function defined by a shape parameter (*Shape*) and a limit parameter (*Limit*). Three values were chosen for each parameter resulting in 9 pairs of parameters for each index. Colored lines represent the shape parameter varying from linear: $Shape = 1.0$ (red), logistic $5.0 < Shape < 30.0$ (green), to step function where $Shape = 500.0$ (blue). Line type represents three different values for *Limit* parameters where references (dashed line) are values of $i_{\text{rd susceptibility}}$, BP_{limb} , act_{limit} and G_{limit} (given in table 4), whereas permissive (full line) and restrictive (dashed dotted) represent a 50% decrease or increase respectively.~~